PNE-902F
FINAL REPORT

Plowshare civil, industrial and scientific uses for nuclear explosives

UNITED STATES ATOMIC ENERGY COMMISSION / PLOWSHARE PROGRAM

NEVADA TEST SITE

DISTRIBUTION STATEMENT A
Approved for Public Release
Distribution Unlimited

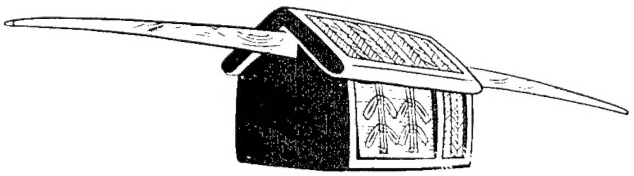

NEVADA CALIFORNIA
MERCURY
LAS VEGAS

Galanquin

Close-in Air Blast from Cratering Nuclear Detonation in Rhyolite

Reproduced From Best Available Copy

Sandia Corporation

Albuquerque, New Mexico

ISSUED: OCTOBER 25, 1968

LEGAL NOTICE

Printed in USA. Price $3.00. Available from the Clearinghouse for Federal Scientific and Technical Information, National Bureau of Standards, U. S. Department of Commerce, Springfield, Virginia 22151.

USAEC Division of Technical Information Extension, Oak Ridge, Tennessee

PNE-902
NUCLEAR EXPLOSIONS-PEACEFUL
APPLICATIONS (TID-4500)

PROJECT PALANQUIN

CLOSE-IN AIR BLAST FROM A CRATERING NUCLEAR DETONATION IN RHYOLITE

L. J. Vortman
Sandia Corporation
Albuquerque, New Mexico

April 1966

ABSTRACT

Close-in air-blast data from the 4.3 ± 0.4 kt Palanquin event in the Plowshare Program for development of nuclear excavation are presented and evaluated. When blast suppression factors are compared with those of past events, an effective yield of 2 kt is required to make Palanquin ground-shock-induced peak overpressures agree with those of past events. Four components of the blast wave from cratering explosions first observed on Project Dugout were again identified on Project Palanquin. The first two, the ground-transmitted, ground-shock-induced pulse and a Rayleigh-wave-induced pulse, are of academic interest. Of primary interest to Plowshare excavation projects are the air-transmitted, ground-shock-induced pulse (which dominated all the others) and the pulse from venting gases (for which the data suggest that peak overpressure may increase as the yield increases).

Close-in pressures should be measured on any future event with a yield equal to or larger than Palanquin to resolve uncertainties created by the nature of Palanquin venting and to determine if there are nonscaling pressure increases with larger yields. The transition region between the epicenter and the genesis of the Rayleigh wave warrants investigation when the opportunity arises.

FOREWORD

"This document is the author's report to the Technical Director of Project Palanquin. The findings and conclusions contained herein are those of the author and are not necessarily those of the Atomic Energy Commission. Accordingly, references to this material must cite the author."

ACKNOWLEDGMENTS

These measurements of the Palanquin air blast were obtained by B. C. Holt. He was assisted in planning and engineering by H. R. Holmes. The data were reduced by J. L. Martinez. J. P. Dietz prepared the playbacks presented herein.

TABLE OF CONTENTS

		Page
CH 1 -	INTRODUCTION	5
1.1	Description of the Palanquin Event	5
1.2	Objectives	5
1.3	Background	6
CH 2 -	PROCEDURE	8
2.1	Experiment Plan	8
2.2	Instrumentation	8
CH 3 -	TEST RESULTS	9
3.1	Summary of Results	9
CH 4 -	DISCUSSION AND INTERPRETATION	13
4.1	Introduction	13
4.2	Ground-Transmitted, Ground-Shock-Induced Pulse	13
4.3	Rayleigh-Wave-Induced Pulse	14
4.4	Air-Transmitted Ground-Shock-Induced Pulse	16
4.5	Flare Pulse	16
4.6	First Positive Phase Impulse	20
4.7	Peak Negative Pressure and Negative Impulse	22
4.8	Pulse from Venting Gases	23
4.9	Total Impulse	24
4.10	Pulse Identification	25
4.11	Discussion	27
CH 5 -	CONCLUSIONS	30
REFERENCES		31
APPENDIX A -	Pressure-Time Records	33

CLOSE-IN AIR BLAST FROM A CRATERING NUCLEAR DETONATION IN RHYOLITE

CH 1 - INTRODUCTION

1.1 Description of the Palanquin Event

Project Palanquin was a nuclear experiment in hard, dry rhyolite rock executed as part of the Plowshare Program for development of nuclear excavation. Palanquin was fired on April 14, 1965, at approximately 0514.0105 (PST), 1314.0105 (GMT), in Area 20, Nevada Test Site. The resultant yield was 4.3 ± 0.4 kt. The emplacement hole was U20K at geodetic coordinates

Longitude	W116° 31' 24.8012"
Latitude	N 37° 16' 49.3501"

The resultant average crater dimensions are:

(1)	Crater Radius	36.31 meters	119.13 feet
(2)	Crater Depth	24.01 meters	78.8 feet
(3)	Crater Lip Height	6.47 meters	21.22 feet
(4)	Lip Crest Radius	44.66 meters	146.53 feet
(5)	Ejecta Boundary	81.63 meters	267.83 feet
(6)	Lip Volume, Apparent	98,757 cubic meters	131,260 yd^3
(7)	Crater Volume, Apparent	35,569 cubic meters	46,802 yd^3

1.2 Objectives

The objectives of the close-in air-blast experiment were:

a. To measure close-in air blast as a function of distance from a nuclear explosion in hard rock at a yield larger than those fired theretofore,

b. To compare these measurements with results from earlier HE and NE detonations in hard rock and other media, and

c. To establish a means for predicting blast from large-yield nuclear explosions by establishing blast suppression as a function of charge burial.

1.3 Background

Close-in air blast from single TNT shots in hard rock (Project Buckboard[1]) showed little difference from that from single TNT shots in alluvial soil (Project Stagecoach[2] and Project Scooter[3]). Both exhibited two waves propagated at sonic velocity in air, one due to the piston action of the ground shock at the epicenter followed by a second larger pulse due to venting gases. Project Danny Boy[4,5], the first nuclear cratering experiment in hard rock (0.43 kt at 115 ft), gave signals in which, by contrast, the initial wave was the larger. Lack of an accurate time base on the records prevented positive identification of larger constituents of the wave. Projects Dugout[6] (a row of five 20-ton nitromethane charges buried 59 ft and spaced 45 ft apart) and Sulky[7] (a single 0.085 kt nuclear charge at 90 ft) records were accurately timed and provided the opportunity for positive identification of four constituents of the blast wave, which were as follows.

a. A ground-transmitted, ground-shock-induced pulse, which is maximum at the epicenter, propagated radially from the explosion at sonic velocity in rock. Because the ground shock attenuates rapidly with distance, so also does the air blast it generates. The attenuation rate of the induced air pulse is further increased because only the vertical component of ground motion will generate air blast, and that component decreases rapidly with decreases in the ratio of burial depth to distance. The direct ground-shock-induced pulse was not positively identified from arrival times on either the Dugout or Sulky shots because of the great spacing between the epicenter and the closest gage. However, it may have been indicated by a larger-than-expected peak overpressure at the closest gage station on each event.

b. A Rayleigh-wave-induced pulse was observed from the closest to the most distant stations on both the Dugout and Sulky events. This pulse propagated in basalt at about 4500 ft/sec--slower than the shock velocity in rock but faster than that in the air. Until the Palanquin event, it was not certain whether this was actually an air-pressure pulse or the output of a gage sensitive to the ground motion.

c. The air-transmitted, ground-shock-induced pulse is, at the epicenter, the same as the ground-transmitted, ground-shock-induced pulse. From the epicenter, however, it propagates outward at shock velocity in air rather than at the velocity through the ground. For Projects Sulky and Dugout, it was the dominant wave, and it is presumed to have been the dominant pulse for Danny Boy.

d. The final pulse is that due to venting gases. On both Sulky and Dugout, the arrival coincided with the negative phase following the preceding air-transmitted, ground-shock-induced pulse. Because

of this and the small amount of gas created by the nuclear explosion, the peak overpressures from the Sulky gas venting pulse did not rise above ambient pressures. For Project Dugout, the peak was greater than the ambient pressure but still was not as large as the peak from the air-transmitted, ground-shock-induced pulse.

In addition to the principle objectives, the Palanquin experiment was designed to shed light on air blast at the epicenter and in the region between the epicenter and the closest previous measurement, especially to identify both the ground-transmitted, ground-shock-induced pulse and the development of the Rayleigh-wave-induced-pulse.

In the formation of the crater from the 280-foot Palanquin shot erosion from venting gases appears to have played a larger part than on previous cratering events. For this reason the air blast from venting gases of Palanquin may not be precisely comparable to that of the earlier shots.

CH 2 - PROCEDURE

2.1 Experiment Plan

One blast line was installed running radially S70°E from ground zero; six stations, each containing two gages, were located at 0, 328, 705, 1575, 3280, and 7380 feet. A third gage was added at the most distant staion with the gage port closed to determine whether or not the gage was measuring a Rayleigh-wave-induced air pressure or was sensitive to the Rayleigh wave itself. The ground zero station consisted of two gages suspended at a height of 3 feet above the concrete pad approximately 21 feet from surface zero. Because of uncertainty in the expected overpressure, each of the two gages had different set ranges (Table 2.1). Thus, if the overpressure was higher than expected, the low range gage would be overranged and the higher range gage would record satisfactorily. Similarly, if the overpressures were small, the lower range gage would record the signal even if it fell below the sensitivity of the higher range gage.

TABLE 2.1

Location and Set Ranges of Gages

Station No.	Range		Expected Overpressure (psi)	
	Feet	Meters	High Range	Low Range
1	21	~6	15	3
2	328	107	0.6	0.2
3	705	215	0.25	0.09
4	1575	480	0.10	0.035
5	3280	1000	0.045	0.015
6	7380	2250	0.020	0.007

2.2 Instrumentation

Pace P-7 diaphragm-type pressure gages were used. Information was carried through Consolidated System D amplifiers with an 800-cps response and recorded with an Ampex LP-100 magnetic tape recording system. There were no gage failures other than those which were anticipated at the ground zero stations when either signal cables broke or the suspended gages came in contact with the rising ground surface.

CH 3 - TEST RESULTS

3.1 Summary of Results

All measured overpressures were at or slightly below the set range of the more sensitive gages. Only the most sensitive gage at ground zero showed evidence of limiting.

Table 3.1 summarizes the results of the pressure measurements. The pressure records are reproduced in Appendix A. As in the two previous experiments (Dugout and Sulky), records from dual-gage stations have been plotted together and the agreement, in spite of the difference in set ranges, is quite good, as evidenced by the similarity of the two records.

The various peaks in certain of the records in Appendix A have been identified where possible by numbers from one to four, according to the four major phases of the blast wave described in Chapter 1. Letters following the numeral indicate the sequence of minor waves in that phase of the wave train. Peak overpressures are similarly identified in Table 3.1.

A flare of hot gas was evidenced by a brilliant flare of light at about 36 milliseconds. The gas came to the surface about 21 feet from the closest gage station, and propagated outward from surface zero at sonic velocity in air, and is seen as a spike on the records at all stations superimposed on the air-transmitted, ground-shock-induced pulse. This spike has been identified in the table and in the records as 3c.

In Figure 3.1, the time-of-arrival of various signals and times of major peaks are plotted versus distance, and the propagation velocity is shown. The ground-transmitted waves are easily distinguished from air-transmitted ones.

With the exception of the two gages at the most distant station, all channels were recorded directly. These two channels were multiplexed with channels from experimental gages. While in principle no differences should have occurred, in fact the amplitudes of those two channels, although in agreement with each other, are about 2-1/2 times higher than would be expected from a comparison with records from other gage stations. This difference was not recognized until long after the event and after a portion of the equipment had been disassembled. An effort to determine a cause of the difference was unsuccessful. Little further comment is made on this inconsistency, and throughout the discussion (Chapter 4) the records from those two gages are ignored in making comparisons.

As noted in Chapter 2, a third gage, with its port sealed to exclude air pressure, was added to the station at 7380 feet. Previous measurements of ground-transmitted, ground-shock-induced and Rayleigh-wave-induced pulses left doubt as to whether induced air pressure was being measured or whether the gage, acting as an accelerometer, was measuring ground motion directly. The gage with the port closed, identical in every other way with one of the others at the same station, produced no detectable signal. On the basis of this measurement, it can be stated as conclusively as a single measurement warrants that the gage is not acceleration-sensitive and is, in fact, measuring air pressure induced by the ground motion.

TABLE 3.1

Summary of Pressure Measurements

Ground Range (ft) and Gage Number	Arrival of First Pulse	Ground-Transmitted, Ground-Shock-Induced Pulse (1)		Rayleigh-Wave-Induced Pulse* (2)		Air-Transmitted, Ground-Shock-Induced Pulse* (3 arb)		Flare Pulse (3c)		Time of Crossover (sec)	Positive Impulse to Crossover (psi-msec)	Negative Peak (psi)	Time of Peak (sec)	Negative Impulse (psi-msec)	Time of Crossover (sec)	Pulse from Venting Gas* (4a & b)			Time of Crossover (sec)	Total Impulse (psi-msec)
		Maximum Peak (psi)	Time of Peak (sec)	Maximum Peak (psi)	Time of Peak (sec)	Maximum Peak (psi)	Time of Peak (sec)	Maximum Peak (psi)	Time of Peak (sec)							Maximum Peak (psi)	Time of Peak (sec)	Positive Impulse (psi-msec)		
21-1 (0)		Peaks Limited - Not Used																		
21-2 (0)	0.0431	5.52	0.049					4.73	0.046		25.6									
328-1	0.0765	0.1810?	0.114	0.2038?	0.131	a. 0.2474 b. 0.1878	0.210 0.302	0.3628	0.333	0.410	57.64	-0.1655	0.6835	54.94	1.160	a. 0.0692 b. 0.0277	1.397 1.789	18.35	1.893	21.05
328-2	0.0805	0.1886?	0.112	0.2069?	0.131	a. 0.2480 b. 0.1949	0.210 0.302	0.4695	0.332	0.409	57.58	-0.1664	0.6970	51.54	1.150	a. 0.0728 b. 0.0323	1.363 1.783	18.73	1.874	24.77
705-1	0.137	0.0009?	0.145	0.0408?	0.201	a. 0.0530 b. 0.0722	0.452 0.6465	0.1512	0.679	0.7575	23.12	-0.0444	1.150	12.65	1.3035	a. 0.0237 b. 0.0219	1.726 2.143	11.54	2.614	22.01
705-2	0.137	0.0011?	0.137	0.0509?	0.202	a. 0.0643 b. 0.0874	0.452 0.645	0.2070	0.677	0.7555	28.24	-0.0556	1.149	15.26	1.299	a. 0.0307 b. 0.0275	1.721 2.143	14.50	2.610	27.48
1575-1	0.390?			0.0020? a. 0.0028 b. 0.0206 c. 0.0071 d. 0.0118	0.440 0.711 0.792 1.003 1.195	a. 0.0195 b. 0.0174	1.342 1.452	0.0598	1.486	1.540 1.748	8.05 9.08	-0.0191	1.971	3.65	2.279	a. 0.0136 b. 0.0161	2.497 2.979	8.31	3.399	12.81
1575-2	0.406?			0.0036? a. 0.0035 b. 0.0200 c. 0.0111 d. 0.0131	0.444 0.713 0.789 1.007 1.193	a. 0.0193 b. 0.0163	1.340 1.455	0.0556	1.484	1.546 1.748	8.84 10.00	-0.0168	1.969	2.44	2.2675	a. 0.0141 b. 0.0162	2.494 2.976	8.80	3.393	15.17
3280-1	0.682			0.0016 a. 0.0025 b. 0.0017 c. 0.00026 d. 0.0021 e. 0.0033	0.742 1.083 1.307 1.629 2.147 2.317	a. 0.0078 b. 0.0062	2.923 2.989	0.0168	3.071	3.097	1.92	-0.0071	3.460	2.39	3.717	a. 0.0048 b. 0.0037	3.988 4.553	1.86	4.698	1.39
3280-2	0.6775			0.0019 a. 0.0029 b. 0.0017 c. 0.00018 d. 0.0021 e. 0.0031	0.7455 1.0875 1.294 1.632 2.1455 2.3115	a. 0.0079 b. 0.0064	2.9155 2.9775	0.0181	3.062	3.089	1.74	-0.0078	3.458	2.55	3.710	a. 0.0049 b. 0.0039	3.980 4.543	1.81	4.693	1.00
7380-1	1.005	0.00075	1.145	0.00048 a. 0.00104 b. 0.00066 c. 0.00117 d. 0.00124 e. 0.00137	1.574 2.114 2.644 3.144 4.074 4.545	a. 0.00579 b. 0.00536	6.715 6.778	0.01554	6.861	6.915	2.90	-0.00341	7.415	0.63	7.508	a. 0.00376 b. 0.00512	7.886 8.360	2.34	8.824	4.61
7380-2	1.005	0.00128	1.1155	0.00061 a. 0.00060 b. 0.00107 c. 0.00113 d. 0.00117 e. 0.00167	1.585 2.135 2.656 3.176 4.086 4.546	a. 0.00529 b. 0.00531	6.714 6.764	0.01407	6.862	6.910	2.54	-0.00335	7.406	0.66	7.504	a. 0.00393 b. 0.00460	7.883 8.363	2.13	8.825	4.01

*See figure in Chapter 3 for blast wave constituents identified in the table by letters.

?Indicates an uncertainty in identification of the peaks.

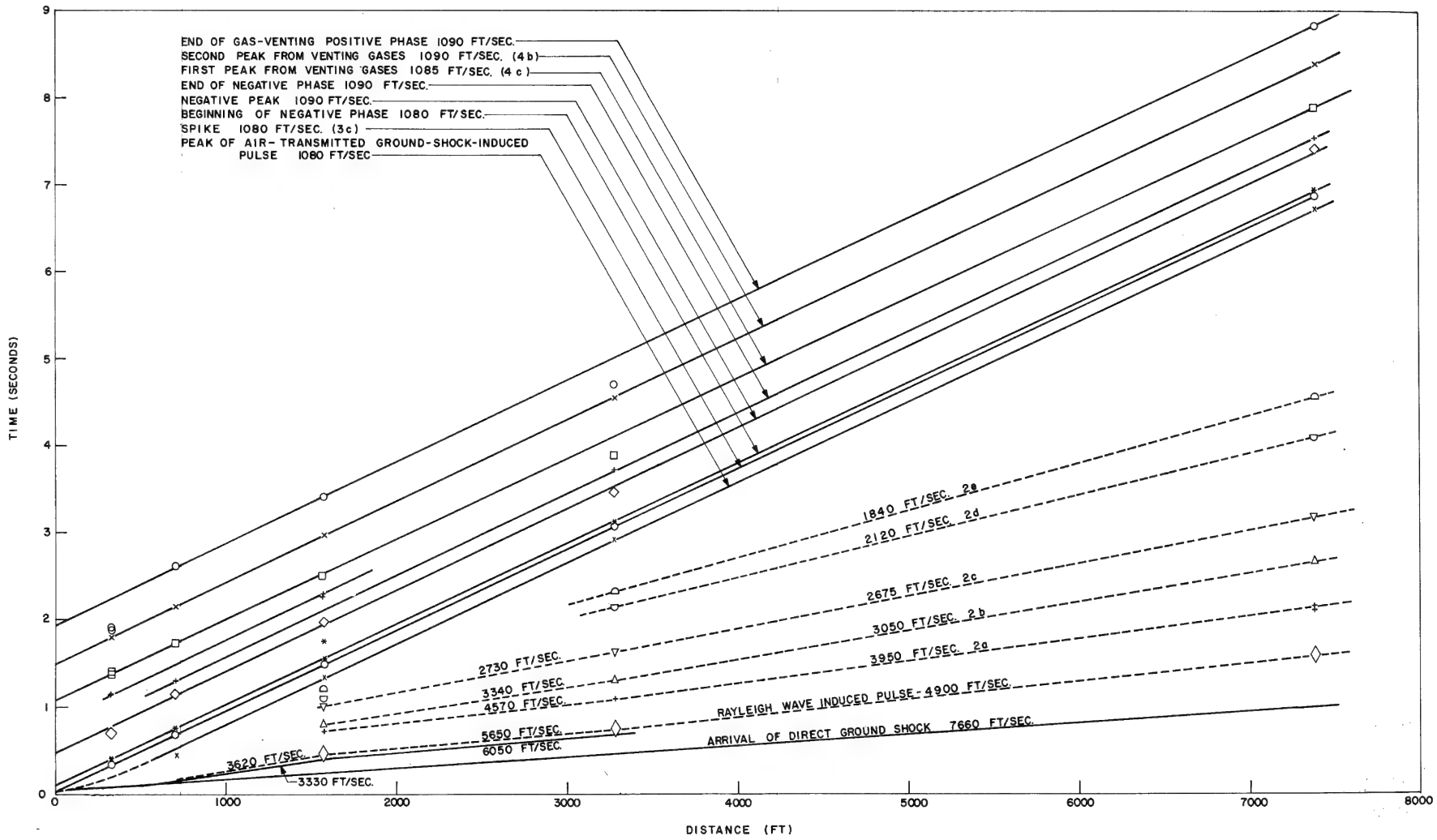

Figure 3.1 Time of arrival versus distance for blast wave components

CH 4 - DISCUSSION AND INTERPRETATION

4.1 Introduction

Chapter 4 is organized to describe fully each of the four pulses in the order of their occurrence. This approach seems more meaningful than to describe all four waves in categories of arrival time, peak overpressures, impulses, and durations.

4.2 Ground-Transmitted, Ground-Shock-Induced Pulse

Arrival Times -- Stearns[9] found the velocity in the upper 90 feet (presumably the weathered zone of the rhyolite) to average 3900 ft/sec. From 90 feet to near shot depth (280 feet) the velocity averaged 8000 ft/sec. Stearn's findings can be used to calculate a maximum arrival time of 46.8 msec for the ground-transmitted wave at the epicenter. Later sonic velocity data, when used in a TENSOR calculation, gave an arrival at about 40 msec.[8] In Table 4.1, the calculated values are compared with measured arrivals. The last two columns suggest that except for the epicenter gage the first arrivals are not those of the ground-transmitted pulse.

TABLE 4.1

Calculated and Measured
Arrival Times of First Signal

Ground Range (ft)	Elevation of Gage (ft)	Calculated Arrival Time (msec)	Measured Arrival of First Detectable Signal (msec)
21	6191	40.* (43.)**	43.1
328	6181.15	68.3	78.5
765	6157.83	111.8	137
1575	6126.38	218.4	398
3280	6093.44	430.8	680
7380	6088.63	945.1	1005

*At the epicenter ground-air interface. An accelerometer record also gave 40 msec.[8]

**At the gage 3 feet above the surface.

One may assume that the free-surface velocity is twice the vertical component of the ground-shock velocity and that the free-surface velocity equals the particle velocity behind the air-shock front generated by the surface motion. TENSOR calculations, which at later times are in agreement with observed surface motion data, show the free-surface velocity to be 10.5 m/sec[8] which would lead to a shock strength of 0.53 psi. This is about equal to the 0.62 psi actually observed at 43. msec. An arrival time at the gage of 43. msec indicates an arrival at the ground surface about 3 msec earlier (40. msec)--earlier than the 46.8 msec at the surface suggested by Stearn's velocities alone. Forty msec is in agreement with TENSOR calculations and is reasonable because higher than sonic velocities in the hydrodynamic region would lead to an expected earlier arrival. On the basis of arrival times, the first signal at the epicenter gage (see Figure A-3) is attributed to the ground-transmitted pulse. The subsequent larger pressures are attributed to a flare, described later in more detail, which appears on the motion picture records at about 36 msec.[8]

At each of the next four stations, the first detectable signal on the record arrives from 15 to 80 percent later than calculated. Its arrival at the most distant station is more nearly the calculated value. One possible explanation is offered. Away from the vicinity of the drill hole at ground zero, the medium may depart drastically from that described by Stearns. A deeper layer with lower sonic velocity could significantly delay the arrival time. This hypothesis requires that the lower velocity layer is again thin below the most distant gage station, causing the signal to be transmitted through deeper high-velocity strata.

Peak Overpressures -- The peak overpressures attributed to the ground-transmitted, ground-shock-induced pulse provide no consistent pattern of attenuation with distance. Radial particle velocities in the ground initially attenuate with distance about as the inverse 2.3 power of radial distance. If the peak overpressures induced by the ground motion attenuated at the same rate (they should be attenuated at a greater rate since only the vertical component of motion should induce overpressure in the air), then only the overpressure measured at the 705-foot station gives a reasonable value--those at the 328- and 7380-foot stations are much too high. The preferred interpretation is that the ground-transmitted, ground-shock-induced pulse was observed only at the epicenter station.

4.3 Rayleigh-Wave-Induced Pulse

Arrival Times -- The ground-transmitted pulse, which is presumably Rayleigh-wave-induced, consists of a train of waves, six of which can be tenuously identified. Greater confidence lies in identification at the more distant stations. At closer stations, it is not nearly so clear that the major overpressure peaks can be identified with those of the more distant stations. If identification is correct, the arrival times of the peaks (Figure 3.1) show that each successive wave in the wave train is propagating at a lower phase velocity. The earliest wave has a velocity of from 4900 to 5630 ft/sec, while the last identifiable wave has a velocity of only 1840 ft/sec.

Peak Overpressures -- Peak overpressures of the first wave (identified by 2 in the figures) attenuate approximately as $r^{-1.85}$ (ignoring the value at the 1575-foot station), a rate which cannot be identified with the rate for any previous corresponding pulses on experiments. Because of phase shifts, the succeeding waves have peaks which do not exhibit any uniform rate of attenuation (Figure 4.1).

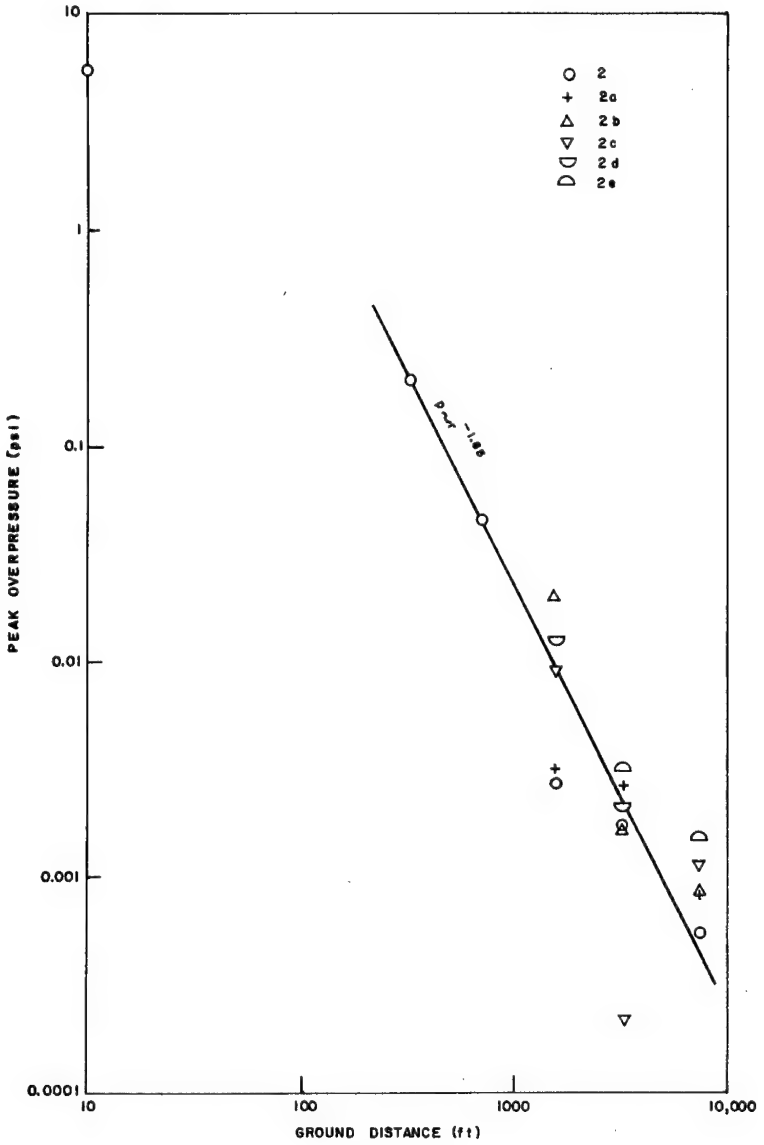

Figure 4.1 Peak overpressure from Rayleigh-wave-induced pulse versus ground distance

4.4 Air-Transmitted Ground-Shock-Induced Pulse

Arrival Times -- The arrival times indicate that the air-transmitted, ground-shock-induced pulse propagates with a velocity (1080 ft/sec) which is in agreement with velocities of other air-transmitted waves (1080-1090 ft/sec). Sonic velocity calculated for the Palanquin ambient conditions is 1084 ft/sec.

Peak Overpressures -- The peak overpressures of the air-transmitted, ground-shock-induced pulse provide a consistent pattern attenuated as $r^{-1.55}$ (Figure 4.2)--except at the most distant station where, as noted earlier, the peaks are more than two times what they should be to be consistent with other stations. Note that peak 3a is equal to or greater than peak 3b except at the 705-foot station. These peaks were the dominant ones at all stations excluding the perturbation of the flare peak described later. Peak overpressures from this pulse have been the most consistent from one shot to the next as contrasted with the peaks from venting gases which are affected by their position in time with respect to the negative phase following the air-transmitted, ground-shock-induced pulse. Because of the consistency, it is in order to ask what yield at the burst depth of Palanquin would have given the observed overpressures. The comparison was made at a scaled range of 5 $ft/lb^{1/3}$ (based on 2 kt), and suggested a yield of 2 kt based on the first peak (peak 3a) and the most sensitive gage at each location. Based on both gages, the suggested yield is essentially the same. By making the comparison on the basis of a ground-shock-induced pulse, any uncertainties resulting from venting anomalies are avoided. Such is not the case if peak overpressures from venting gases are used. The attenuation rate with distance of any air-transmitted pulse such as this peak overpressure is a function of nearly hemispherical divergence modified by meteorological conditions at shot time, especially wind and temperature gradients. Hence, the yield as calculated in this way will depend to some extent on the ground range at which the comparison is made. A scaled range of 5 $ft/lb^{1/3}$ was chosen for the comparison made here only because data at that distance are available for the largest number of shots.

4.5 Flare Pulse

A flare of hot gas gave rise to a true shock wave. Such a wave propagates to all stations at the sonic velocity in air (Figure 3.1) and rides on the declining portion of the air-transmitted wave generated by the epicenter ground shock. The peak flare overpressure as a function of distance is shown in Figure 4.3. The peak overpressures and the impulses of the flare pulse measured with respect to the wave on which the pulse was superimposed are listed in Table 4.2 and plotted in Figures 4.4 and 4.5.

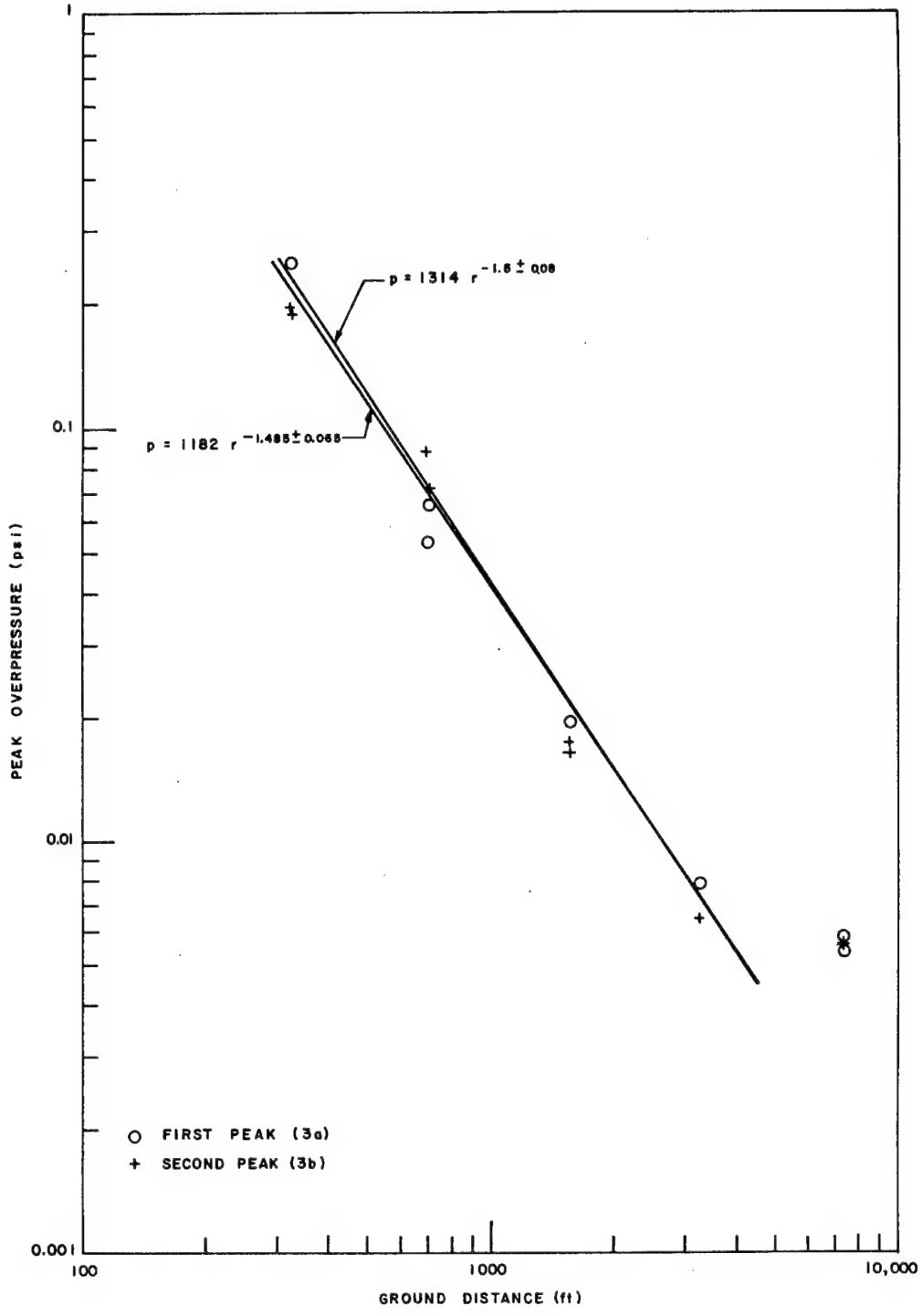

Figure 4.2 Peak overpressure from the air-transmitted, ground-shock-induced pulse versus ground distance

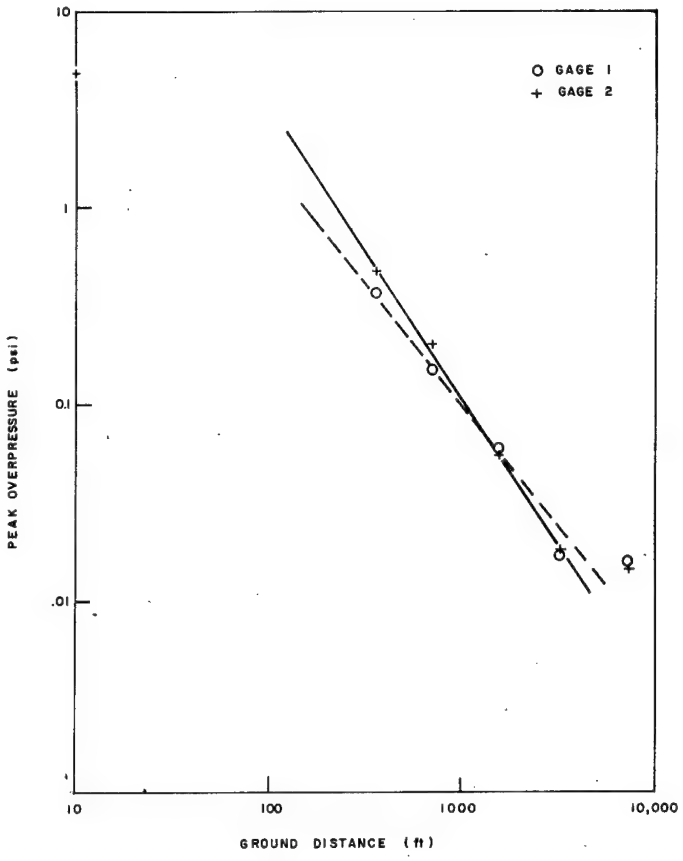

Figure 4.3

Peak flare overpressure versus ground distance

TABLE 4.2

Characteristics of Flare Pulse

Station	Peak Overpressure (psi)	Positive Impulse (psi-msec)	Duration of Positive Phase (msec)
328-1	0.22557	2.80	2.42
-2	0.32966	2.65	3.73
705-1	0.09810	1.01	2.91
-2	0.13824	1.11	3.74
1575-1	0.04665	0.617	2.27
-2	0.04252	0.542	2.35
3280-1	0.01462	0.227	1.93
-2	0.01597	0.293	1.64
7380-1	0.01260	0.146	2.59
-2	0.01157	0.132	2.63

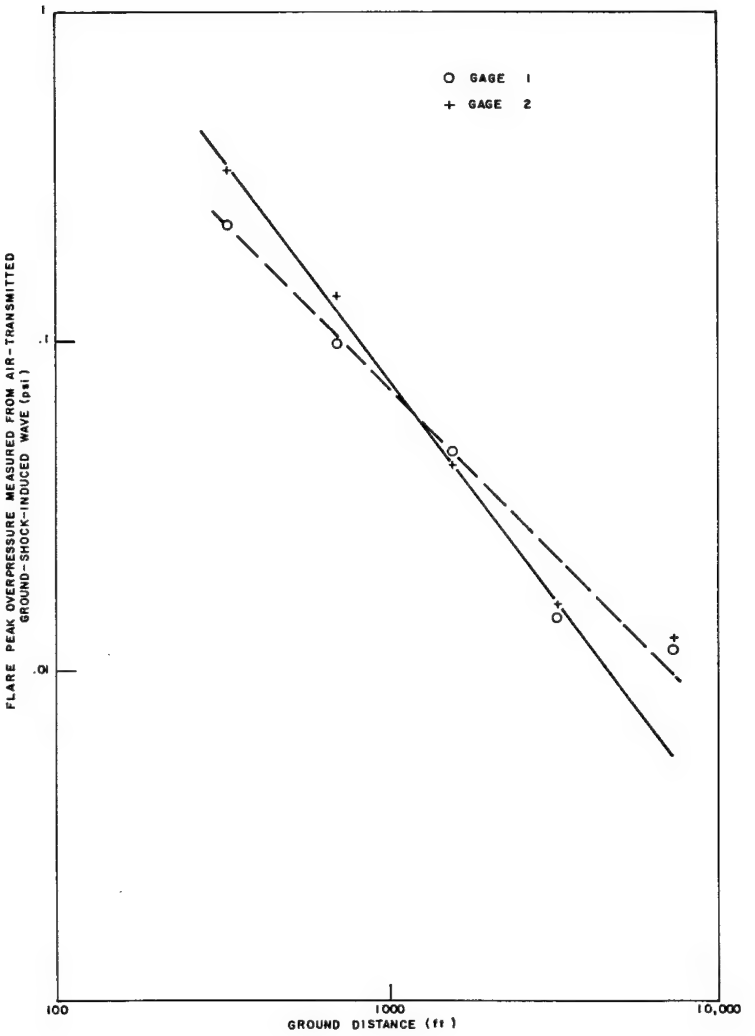

Figure 4.4 Increase in overpressure caused by flare versus ground distance

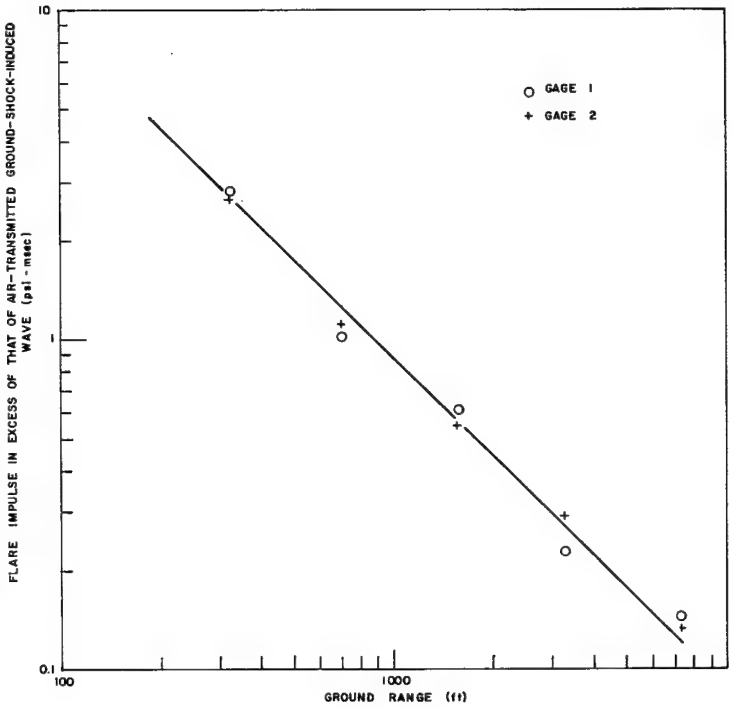

Figure 4.5 Increase in positive-phase impulse caused by flare versus ground distance

High-speed motion pictures recorded arrival at the surface of the flare at 36 msec.[8] The pictures were substantiated by a signal on the electrical system of an accelerometer located nearby. An initial overpressure peak of 4 psi was observed at 45 msec (Figure A-3). About 2.75 pounds of TNT burst on the surface would give 4 psi 21 feet away,[11] and the signal would arrive at about 11.4 msec. This, added to the observed arrival of the flare, suggests the wave would be expected at about 47.4 msec--later than the 45 msec at which it was actually observed. Thus, the arrival time appears consistent only with a stronger shock than that recorded. One possible explanation is that an air shock preceded the flare by about 2.4 msec and that it was not visible on the photographs which recorded the flare.

When the impulse data are extrapolated back to the vicinity of the epicenter, the 25.6 psi-msec measured there (see Figure A-3) is a seemingly reasonable value and suggests that the flare pulse makes the predominant contribution to the pulse measured at the epicenter. The duration of the flare pulse observed photographically was about 11 msec,[10] agreeing with the duration from Figure 4.3.

When the pressure data are extrapolated back to the 2-psi level assuming the attenuation rate of the dashed line of Figure 4.4 and compared with Kirkwood-Brinkley free-air curves for cast TNT, the most sensitive gages (Gage 1, Figure 4.4) suggest an equivalent TNT source of 56 pounds, and the least sensitive gages suggest a source of 150 pounds. Impulse comparison suggests an equivalent source of 3650 pounds.

Since the flare pulse is a shock wave, it can be described by

$$p = p_m\left(1 - \frac{t}{t_+}\right) e^{-c(t/t_+)}$$

where p is the pressure at any time t, p_m the peak overpressure, and t_+ the positive phase duration. The constant c describes the rate of decay of the blast wave. Comparison of this wave-shape factor for the flare pulse with factors for ideal blast waves from HE shows the wave shape to be about that of an ideal blast wave. The constant c has an average value of 0.86 for the flare pulse; this suggests a decay rate slower than most shock waves, and is consistent with the larger equivalent source derived from impulse.

4.6 First Positive-Phase Impulse

The wave train consisting of the first three waves (ground-transmitted, ground-shock-induced; Rayleigh-wave-induced; and air-transmitted, ground-shock-induced) has intermittent excursions below ambient pressure. The summation of impulse to a give time is one means of measuring the consistency of the data. Since the air-transmitted, ground-shock-induced pulse is followed by a distinct negative phase, the crossover preceding the negative phase constitutes a definable time at which to measure impulse. The results (Figure 4.6) show impulse attenuates with distance about $r^{-1.25}$, based on

the second (least sensitive) gage at each of the 328-, 705-, and 1580-foot stations. The positive phase at the 3280-foot station is low with respect to the closer stations. At first glance, it appears caused by a phase shift in which the small pulse immediately following the flare spike moves from the positive phase at the 1580-foot station into the negative phase at the 3280-foot station. As a matter of fact, this pulse could account for only a small portion of the loss of impulse at the latter station. The shift of the small pulse into the negative phase should reduce the negative phase as well and, as will be seen in the following section, such is not the case.

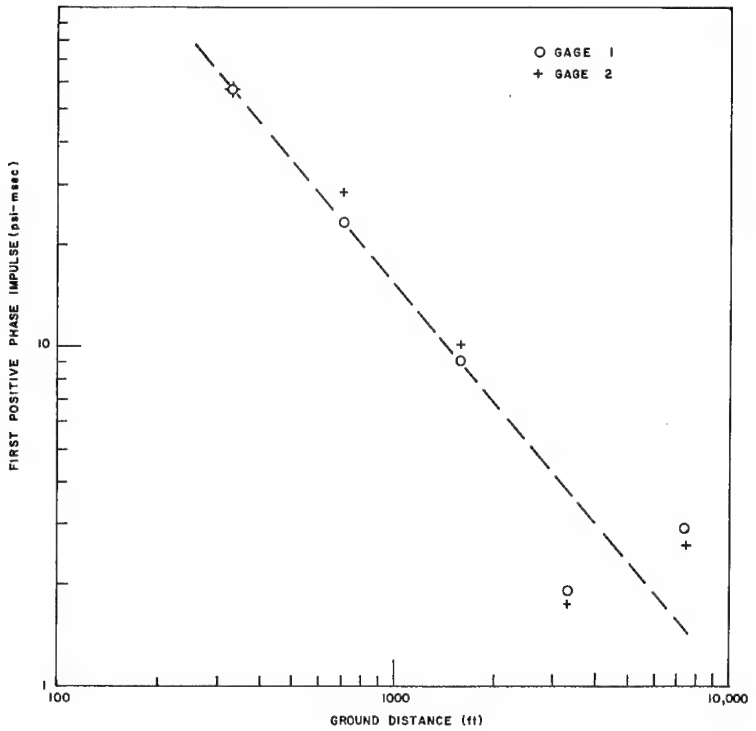

Figure 4.6 First positive-phase impulse versus ground distance

The flare overpressure peaks (Figures 4.3 and 4.4) measured by the less sensitive gages (dashed line) suggest that values for the 3280-foot station are low, but that those measured by the more sensitive gages (solid line) suggest no shortcoming at the 3280-foot station. Flare impulse at the 3280-foot station is consistent with that at the closer station. It would not be consistent if there were a gage calibration error; a base-line drift is a remaining possibility.

4.7 Peak Negative Pressure and Negative Impulse

Peak negative pressure attenuates uniformly with distance (Figure 4.7). Pressures measured at the 3280-foot station are consistent with pressures measured at the closer stations. Negative impulses at that station are definitely high (Figure 4.8). Low positive-phase and high negative-phase impulses strongly suggest a base-line drift upward for both gages at that station. However, that hypothesis is not consistent with a negative peak which agrees well with results at closer stations.

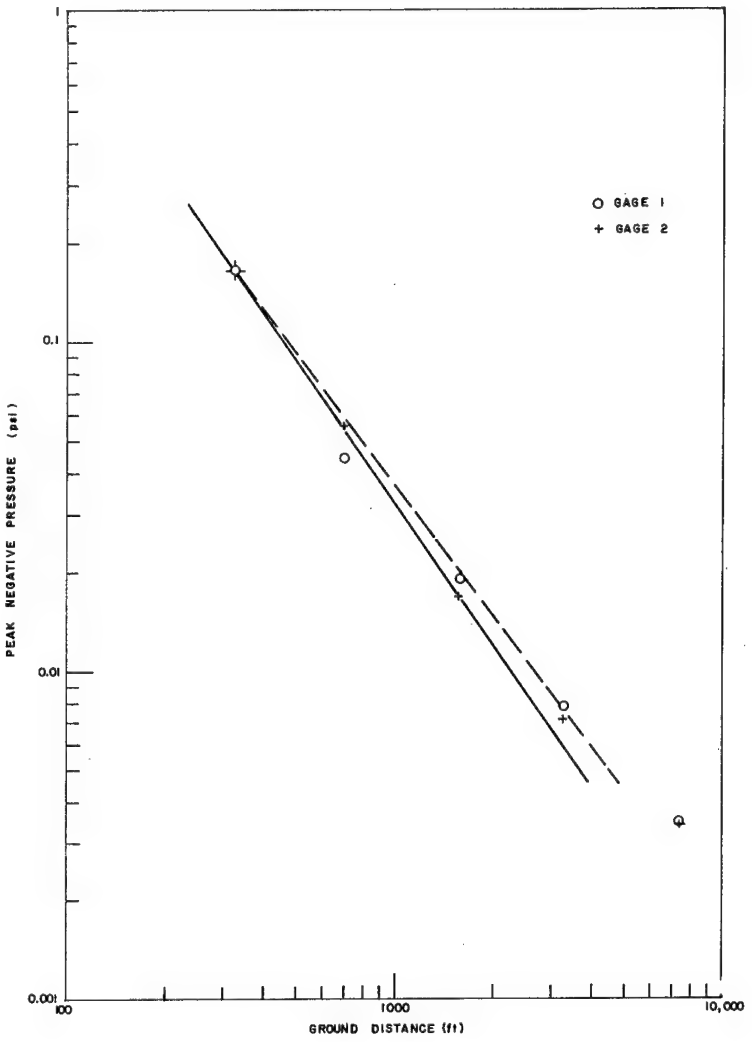

Figure 4.7 Peak negative pressure versus ground distance

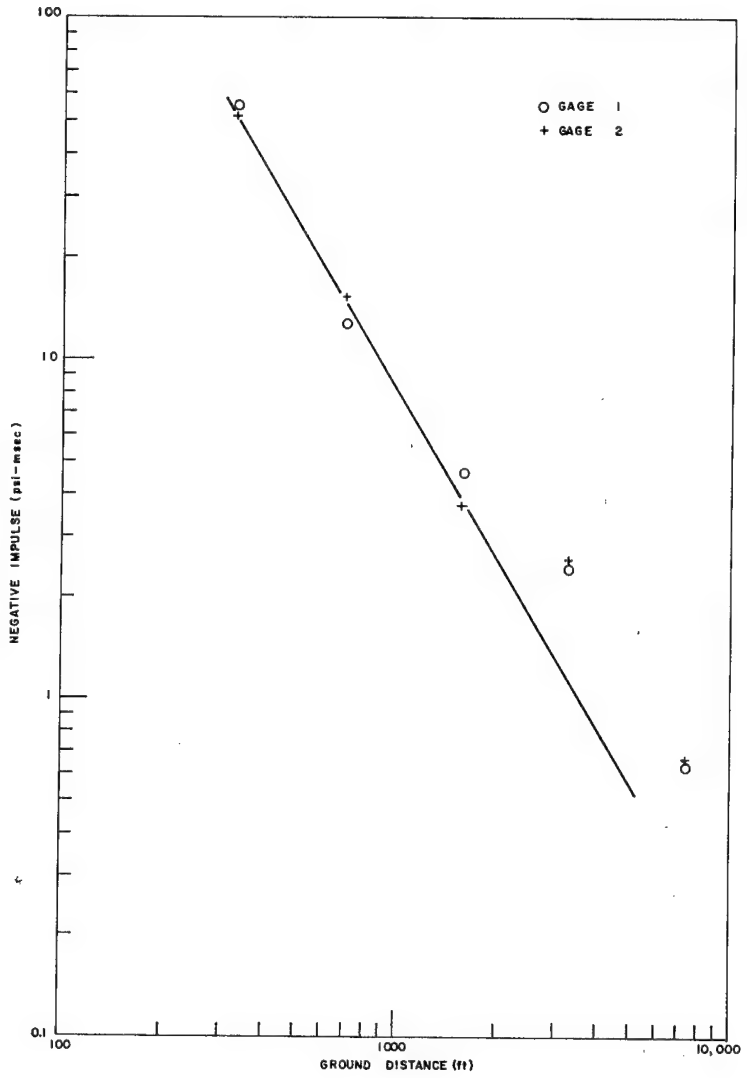

Figure 4.8 Negative-phase impulse versus ground distance

4.8 Pulse From Venting Gases

At all stations except the one near the epicenter, the pulse from venting gases exhibits two distinctly separate pulses (4a and 4b in Figure 4.9 and in figures in the Appendix). Two distinct surges of venting gases are to be seen in the motion pictures of the event, one beginning at 645 msec and one at 837 msec. When the times at which pulse 4a begins to emerge from the negative phase are extrapolated back to surface zero, the agreement with the first of

the above times is good. The 837 msec appears to be too early to be identified with pulse 4b. Certain observations can be made from Figure 4.9. At the 328-foot station, peak 4a is larger than peak 4b by a factor of 2. Further out, however, 4b has attenuated much less and the peaks become nearly equal. Peak 4a attenuates with distance about as the other peaks, and again values for both peaks at 3280 feet appear low with respect to the line shown in the figure which was drawn through values for the more sensitive gages (Gages 2) at stations closer than 3280 feet.

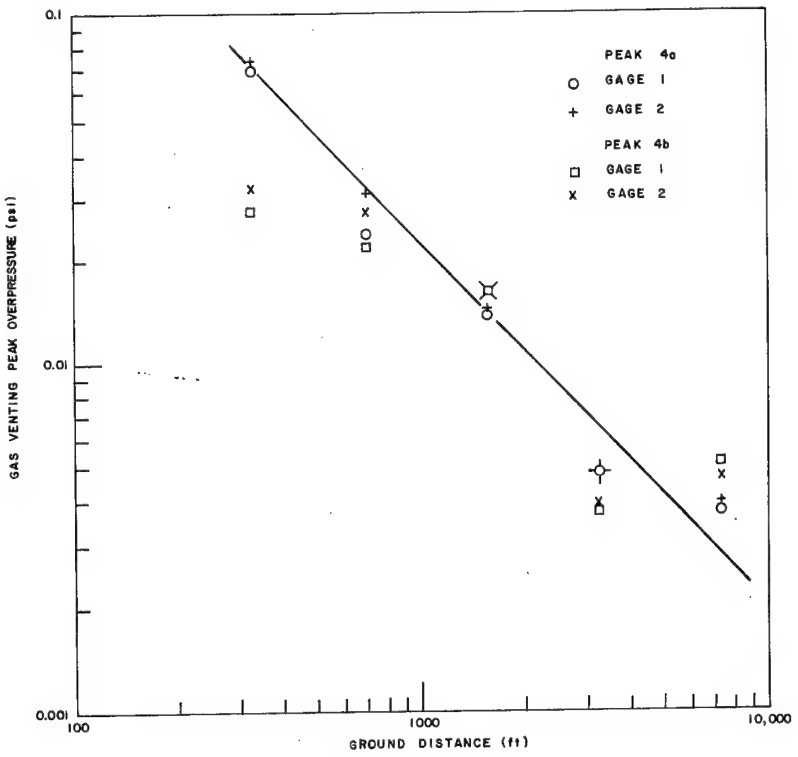

Figure 4.9 Peak overpressure from venting gases versus ground distance

4.9 Total Impulse

Total impulse for the entire wave train from first arrival continues to show low values for the 3280-foot station (Figure 4.10). Values at the near station also appear low, mainly because of the relatively small contribution of pulse 4b at that station.

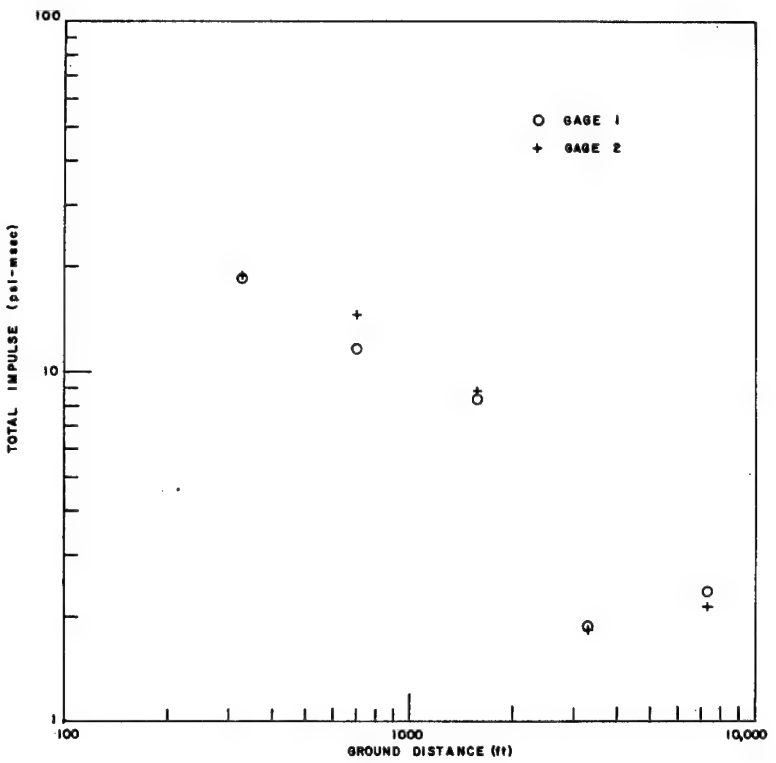

Figure 4.10 Total impulse versus ground distance

4.10 Pulse Identification

An aid to wave identification was found in some auxiliary measurements. Pressure gages identical to those on the ground had been located 35 feet above the 3280-foot station to provide pressure correlation with some experimental gages. Unfortunately, the calibration of these gages was lost, but when the flare peaks were made identical to those measured at ground level, the results are as shown in Figure 4.11. The figure shows a delay of about 35 milliseconds for pulses that are ground-transmitted but little or no delay for those which are air-transmitted. There are some interesting and unexplained qualitative differences between the two signals. The gage 35 feet above ground level shows little of the decrease preceding and following the flare pulse. The steps following the negative peak are noticeably different.

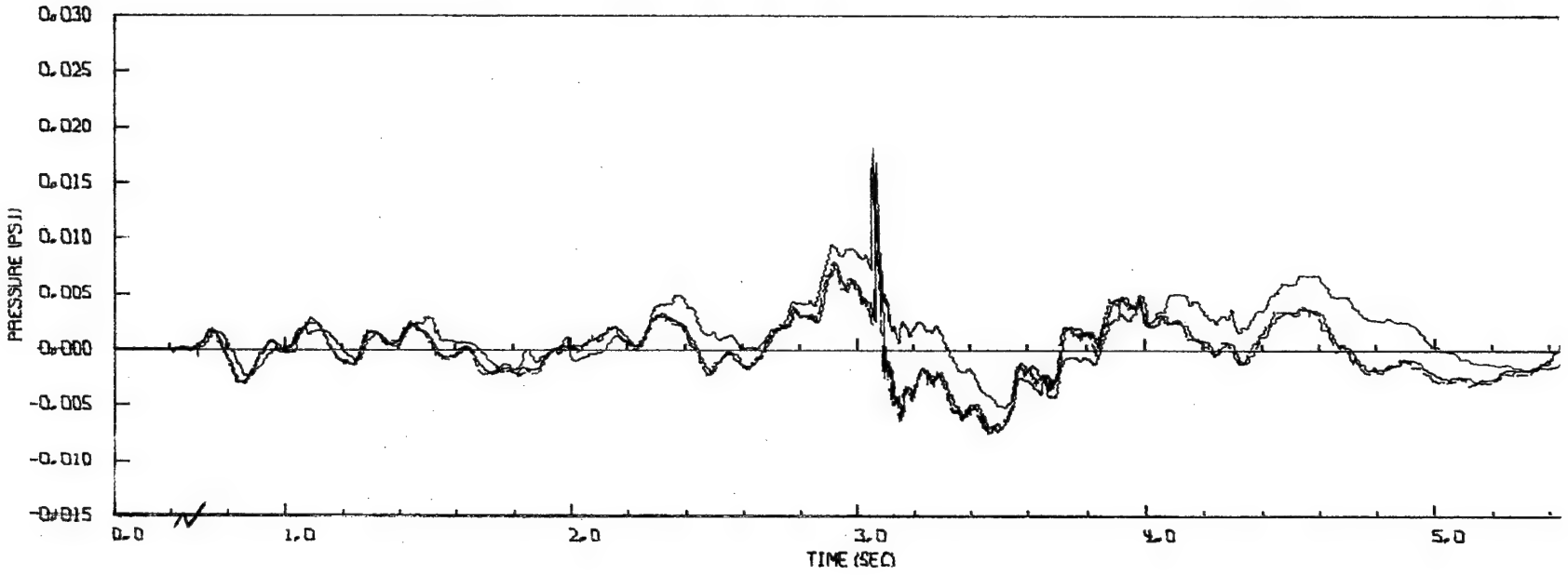

Figure 4.11 Pressure-time record for two surface gages and one gage 35 feet above the surface

4.11 Discussion

While the various pulses in the Palanquin wave train are academically interesting, the major pulses of concern for the Plowshare Program are the air-transmitted, ground-shock-induced pulse and the pulse from venting gases. It is important to inquire into the scaling of air blast from buried nuclear explosions. Air-transmitted, ground-shock-induced pulses from past shots show little difference between HE and nuclear explosions and little difference due to medium--the overpressures are only slightly higher for the harder materials. From earlier shots, the amount of blast suppression by charge burial has been determined. The blast suppression factor is defined here as the ratio of: (a) peak overpressure from a surface burst, and (b) peak overpressure from the same yield buried below the surface.

Figure 4.12 summarizes air-blast suppression by charge burial for all past events at a scaled ground range of 5 $ft/lb^{1/3}$ (630 $ft/kt^{1/3}$). The following are the significant points from Figure 4.12.

a. Peaks from venting gases of nuclear shots in alluvium are suppressed less rapidly by burial than are HE shots. This observation comes from Teapot ESS and Sedan data and can be a result of more pressure caused by water vapor in the medium, or it can be caused by a yield effect--larger yields producing relatively more overpressure. The 100-kt Sedan shot had pressures from venting gases so large that the ground-shock-induced pressures were overtaken by them.

b. What happens to peaks from venting HE gases for bursts deeper than 1.75 $ft/lb^{1/3}$ (220 $ft/kt^{1/3}$) remains to be determined from additional HE experiments at those depths.

c. The ground-shock-induced peaks for HE in both basalt and alluvium and for NE in basalt are essentially the same. The rate of suppression with burial depth of the ground-shock-induced peaks approaches, for the deeper burial depths, the rate of suppression for the peaks from venting gases for HE shots.

d. Information on peaks from venting gases from nuclear events in rock has been limited to Sulky, Danny Boy, and, now, Palanquin. Both of the earlier shots show peaks from venting gases much less than the ground-shock-induced peaks. While the gas-venting peaks were readily identifiable, especially on Sulky, they were superimposed on the negative phase following the ground-shock-induced peaks. As a result, the amplitudes were low (the peaks for Sulky equaled only ambient pressure and yielded an infinity value for the blast suppression factor).

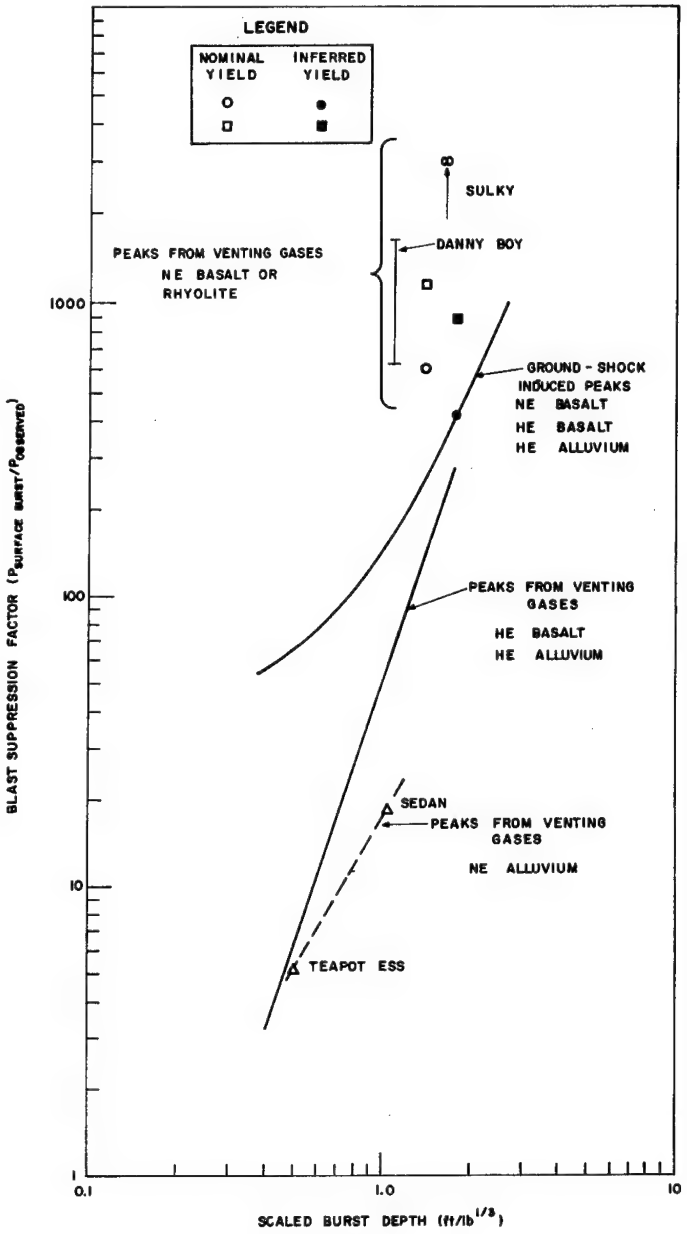

Figure 4.12 Summary of air-blast suppression by charge burial

As noted earlier, when the Palanquin ground-shock-induced overpressures are compared with those of other shots, a yield of 2 kt is indicated. The suppression factors for both peaks and for both the inferred and nominal yields are plotted in Figure 4.12. If the inferred and nominal yields of Palanquin are assumed, the peak overpressure from venting gases at a scaled range of 5 ft/lb$^{1/3}$ for the three nuclear events in rock is as follows.

	W (kt)	dob (ft/lb$^{1/3}$)	P_{max} (psi)
Sulky	0.085	1.66	0
Danny Boy	0.43	1.15	0.015 - 0.040
Palanquin	2.00	1.76	0.028
Palanquin	4.00	1.40	0.022

There remains in these data a suggestion of an increase in pressure from venting gases with an increase in yield. Since there is also a suggestion of an increase with deeper scaled burial depth, the increase with yield for a single burial depth would be even more pronounced. If further data verify the increase with yield, the very large peaks from venting gases from Sedan would have a clearer basis than higher moisture content alone.

Where the pulse from venting gases is superimposed on the negative phase following the ground-shock-induced pulse, it is impossible to tell whether or not the negative phase reached its natural minimum value before arrival of the pulse from venting gases (or whether arrival of that pulse terminates further excursion into the negative regime by its arrival). If not, the peak-to-peak value is a better measure of the contribution from venting gases than the overpressure. The results of Sulky and Palanquin (no negative pressures are available for Danny Boy) at a scaled range of 5 ft/lb$^{1/3}$ are

	W (kt)	dob (ft/lb$^{1/3}$)	$P_+ + P_-$ (psi)
Sulky	0.085	1.66	0.038
Palanquin	2.00	1.76	0.108
Palanquin	4.00	1.40	0.076

The suggestion of an increase in pressure contribution from venting gases with an increase in yield remains in the peak-to-peak pressures also. Motion pictures of the venting of gases from Palanquin suggest characteristics which are qualitatively different from previous explosions at comparable burial depth. Consequently future experience may show that comparisons such as those made above are invalid.

CH 5 - CONCLUSIONS

Four separate components of the blast wave were identified. These were: a ground-transmitted, ground-shock-induced pulse; a Rayleigh-wave-induced pulse; an air-transmitted, ground-shock-induced pulse; and a pulse from venting gases. The latter two pulses are the ones of primary interest to Plowshare excavation projects. For Palanquin, the air-transmitted, ground-shock-induced pulse dominated the other pulses. The pulse from venting gases was smaller primarily because it was coincident with the negative phase immediately following the air-transmitted, ground-shock-induced pulse. Otherwise it would have been the dominant pulse. When the peak pressure from Palanquin venting gases is compared with corresponding peaks from comparable explosions, there is tenuous evidence that the peak overpressure increases as the yield increases. Thus, no opportunity should be lost to make comparable measurements on shots with yields larger than that of Palanquin. The manner in which the Palanquin explosion vented was sufficiently unique to make it impossible to compare confidently the pulses from venting gases with corresponding pulses from other buried explosions. For this reason similar measurements should be made on any event with a yield comparable to that of Palanquin. Nothing, however, should impair the credibility of the air-transmitted, ground-shock-induced pulse observed at stations beyond the epicenter.

When the air-transmitted, ground-shock-induced peak overpressures are compared with those from other buried explosions, an effective yield of 2 kilotons is indicated for Palanquin.

The first two pulses are of considerable academic interest. It is not at all clear from the results to date how the transition from the ground-transmitted, ground-shock-induced pulse to the Rayleigh-wave-induced pulse is accomplished. This transition region is worthy of further exploration when the opportunity occurs.

REFERENCES

1. L. J. Vortman, et al, 20-Ton and 1/2-Ton High Explosive Cratering Experiments in Basalt Rock, Project Buckboard, SC-4675 (RR), Sandia Corporation, Albuquerque, New Mexico, November 1960.

2. L. J. Vortman, et al, 20-Ton HE Cratering Experiment in Desert Alluvium, Project Stagecoach, SC-4596 (RR), Sandia Corporation, Albuquerque, New Mexico, January 1962.

3. W. R. Perret, et al, Project Scooter Final Report, SC-4602 (RR), Sandia Corporation, Albuquerque, New Mexico, October 1963.

4. M. D. Nordyke and W. R. Wray, Preliminary Summary Report, Project Danny Boy, UCRL-6999, Lawrence Radiation Laboratory, Livermore, California, July 1962.

5. L. J. Vortman, Close-In Air Blast from a Nuclear Detonation in Basalt, Project Danny Boy, WT-1810, Sandia Corporation, Albuquerque, New Mexico, September 15, 1962.

6. L. J. Vortman, Close-In Air Blast from a Row Charge in Basalt, Project Dugout, Final Report, PNE-608-F, Sandia Corporation, Albuquerque, New Mexico, August 4, 1965.

7. L. J. Vortman, Close-In Air Blast from a Relatively Deep Low-Yield Nuclear Detonation in Basalt, Project Sulky, Final Report, PNE-711F, Sandia Corporation, Albuquerque, New Mexico, to be published.

8. B. Crowley and T. Crawford, A Preliminary Report on Close-In Air Blast--Palanquin, UCID-5075, Lawrence Radiation Laboratory, Livermore, California, October 25, 1965.

9. K. T. Stearns, Seismic Up-Hole and In Situ Velocity Survey in WES, Hole No. 1, U20K Palanquin, Nevada, Lawrence Radiation Laboratory, March 24, 1965.

10. J. B. Knox, verbal communication.

11. L. N. Kingery, J. H. Keefer, and J. D. Day, Surface Air-Blast Measurements from a 100-Ton TNT Detonation, BRL MR-1410, Ballistic Research Laboratories, Aberdeen Proving Ground, Maryland, June 1962.

APPENDIX A

Pressure-Time Records

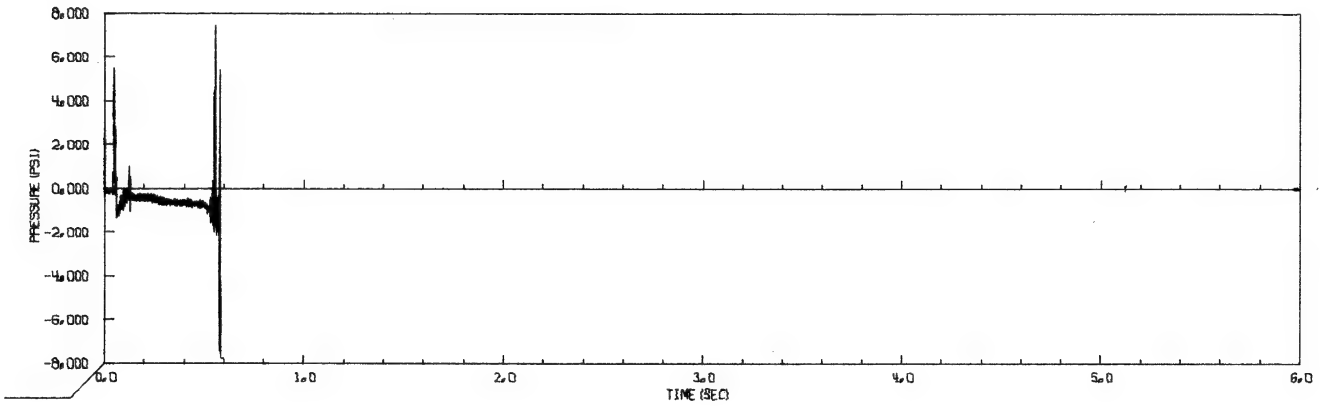

Figure A-1 Pressure-time record from the epicenter station

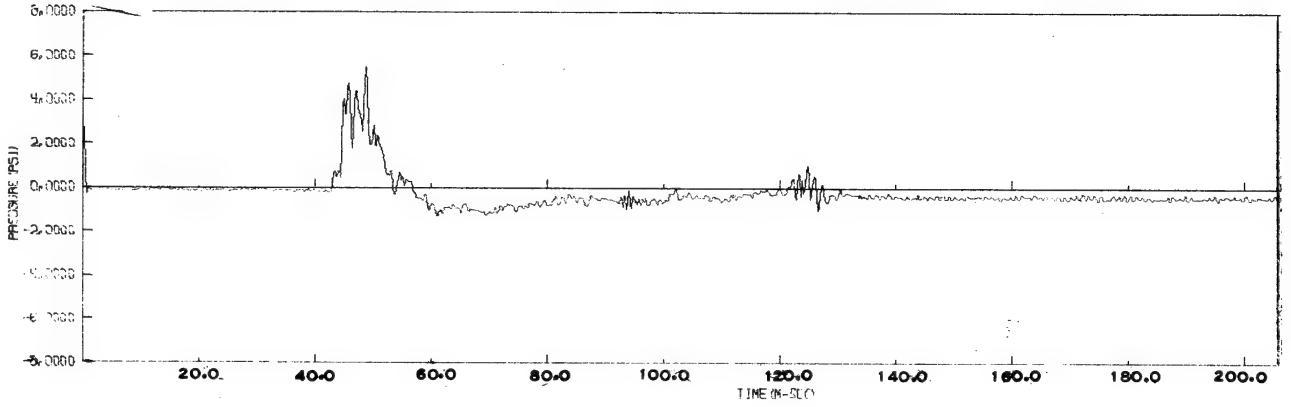

Figure A-2 Expanded pressure-time record from the epicenter station

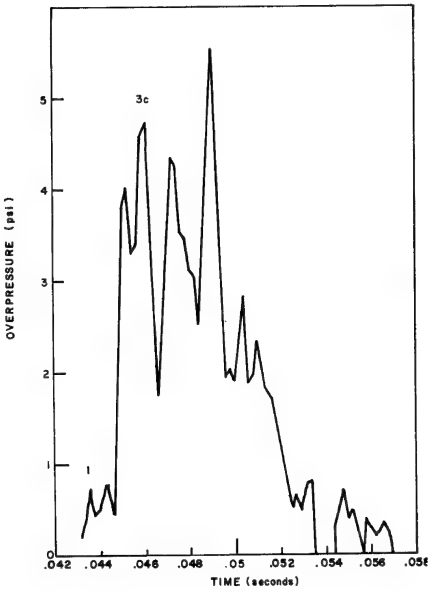

Figure A-3 Expanded pressure-time record from the epicenter station

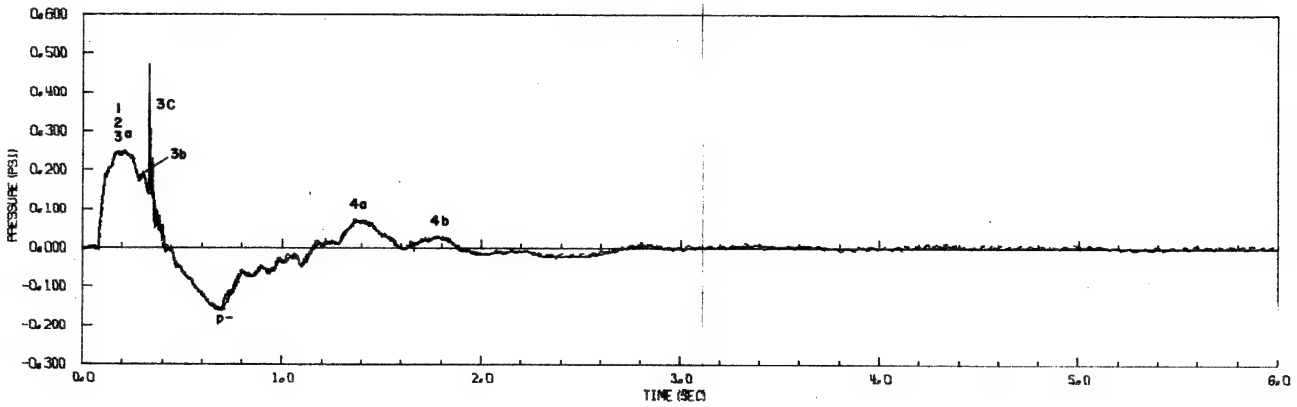

Figure A-4 Pressure-time records from the station at 328 feet (2 gages)

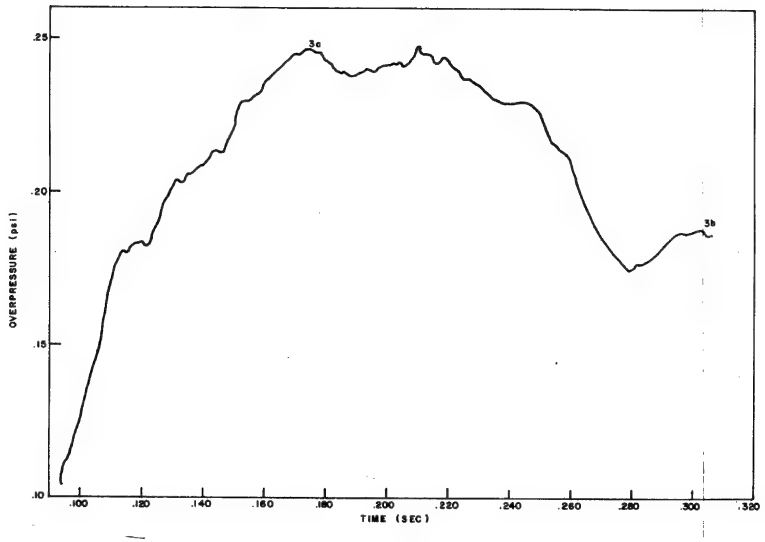

Figure A-5

Expanded pressure-time records from the station at 328 feet (2 gages)

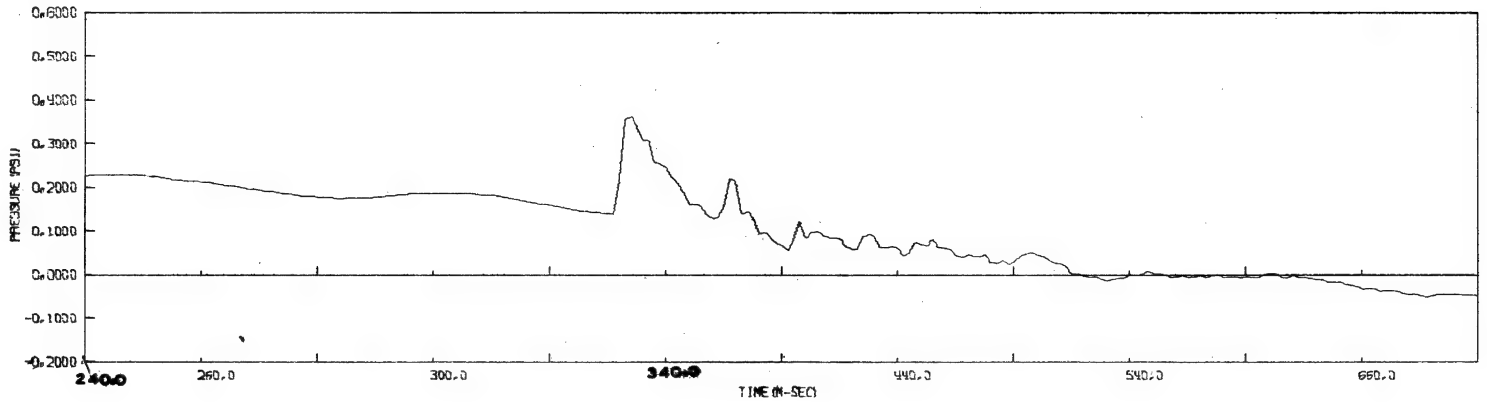

Figure A-6 Expanded pressure-time records of flare pulse from the station at 328 feet (Gage 1)

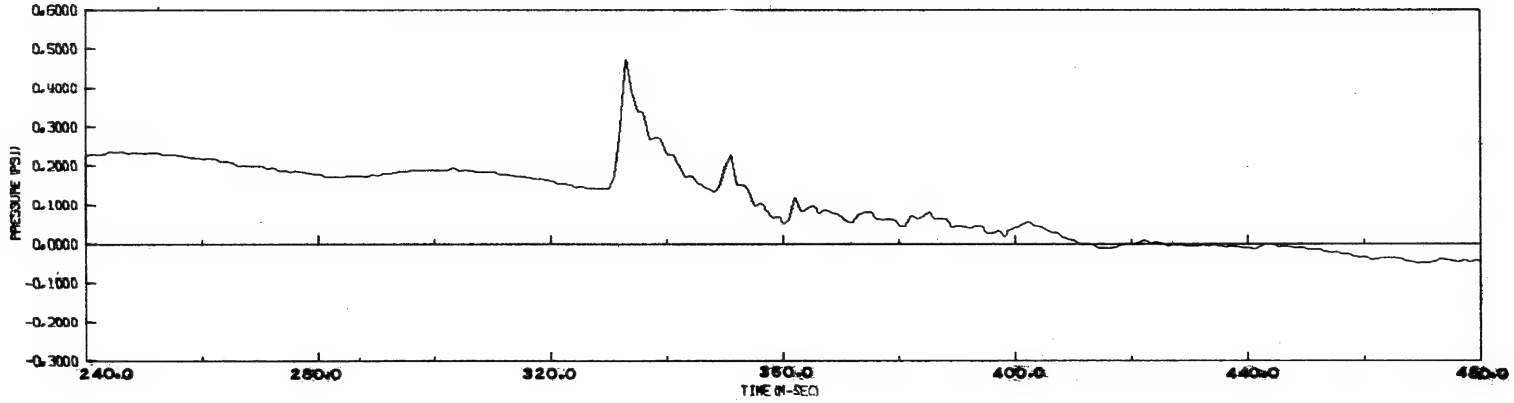

Figure A-7 Expanded pressure-time records of flare pulse from the station at 328 feet (Gage 2)

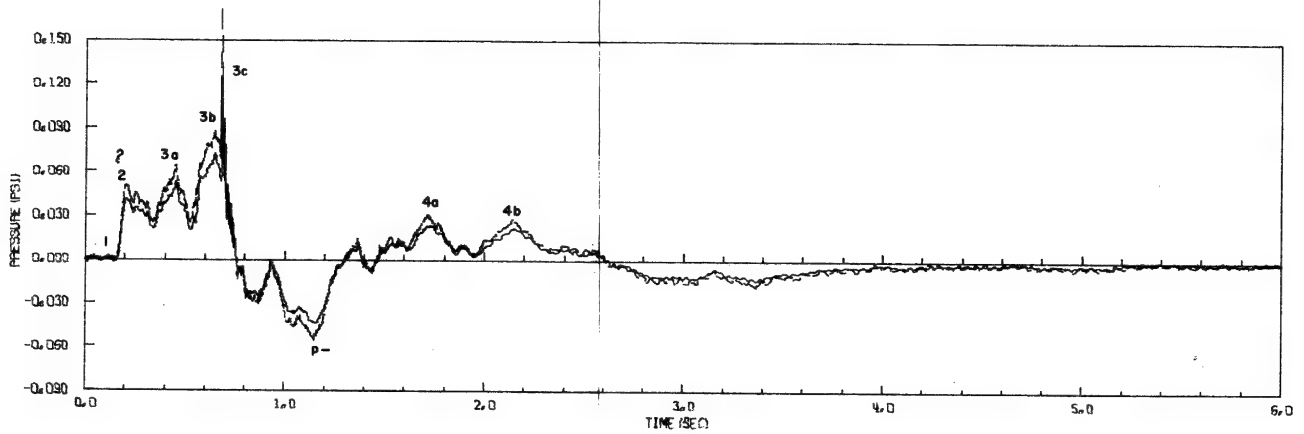

Figure A-8 Pressure-time records from the station at 705 feet (2 gages)

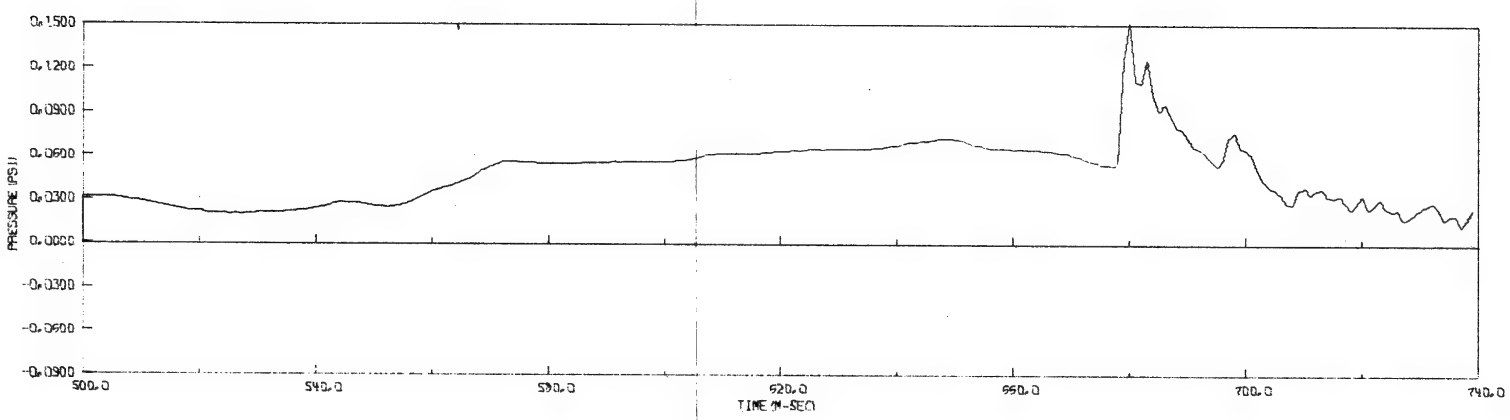

Figure A-9 Expanded pressure-time records of flare pulse from the station at 705 feet (Gage 1)

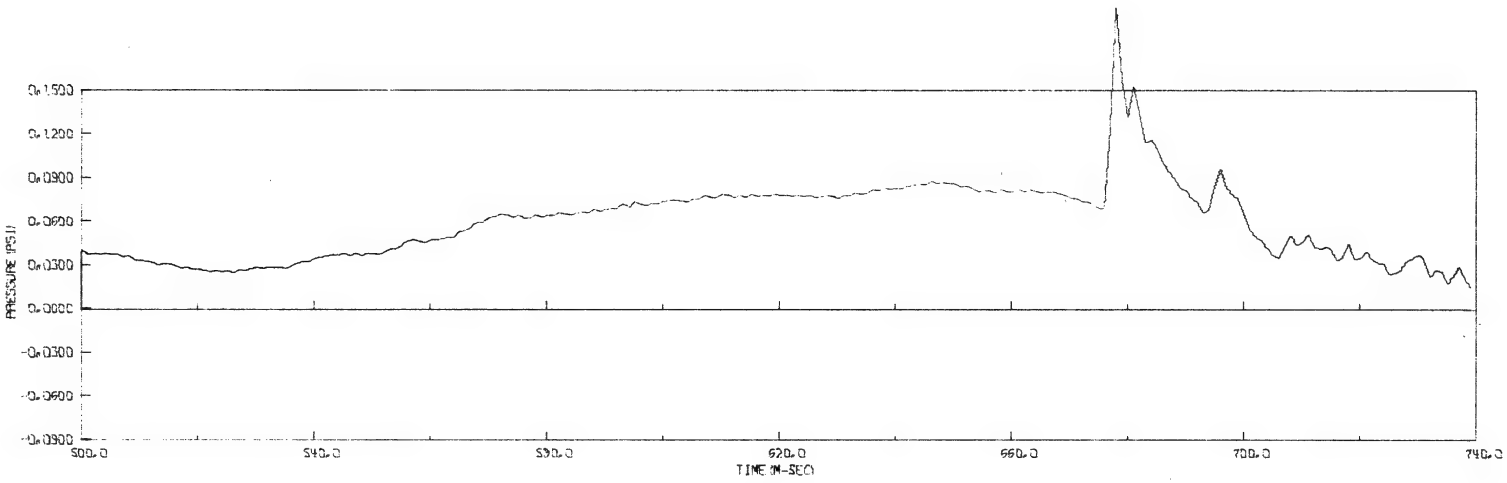

Figure A-10 Expanded pressure-time records of flare pulse from the station at 705 feet (Gage 2)

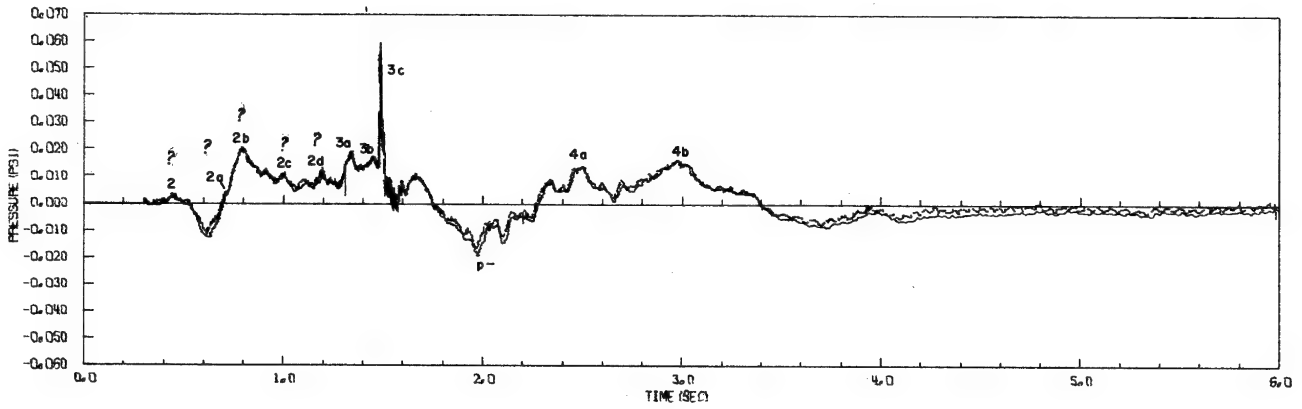

Figure A-11 Pressure-time records from the station at 1575 feet (2 gages)

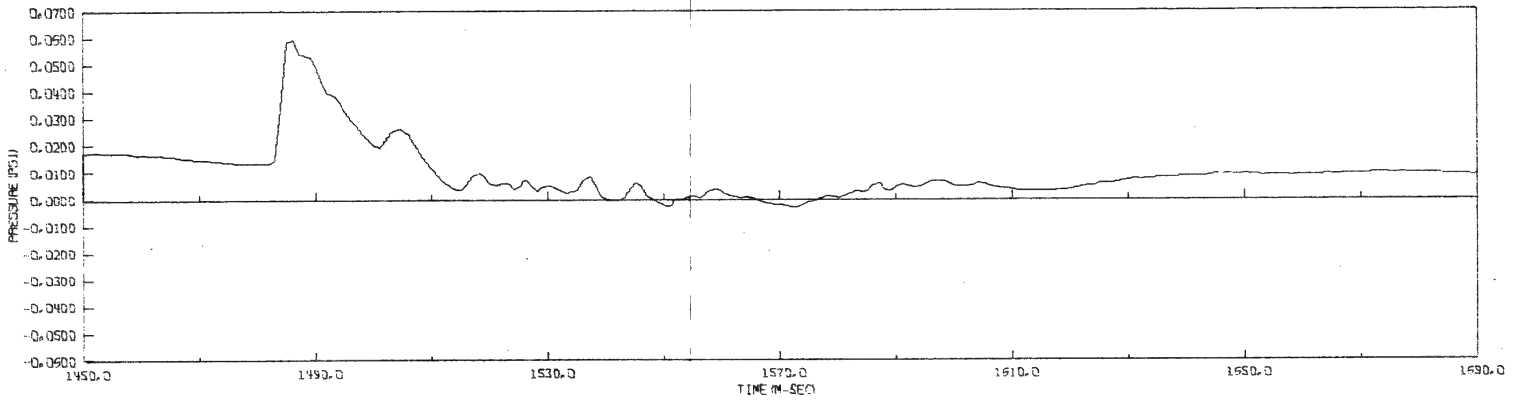

Figure A-12 Expanded pressure-time records of flare pulse from the station at 1575 feet (Gage 1)

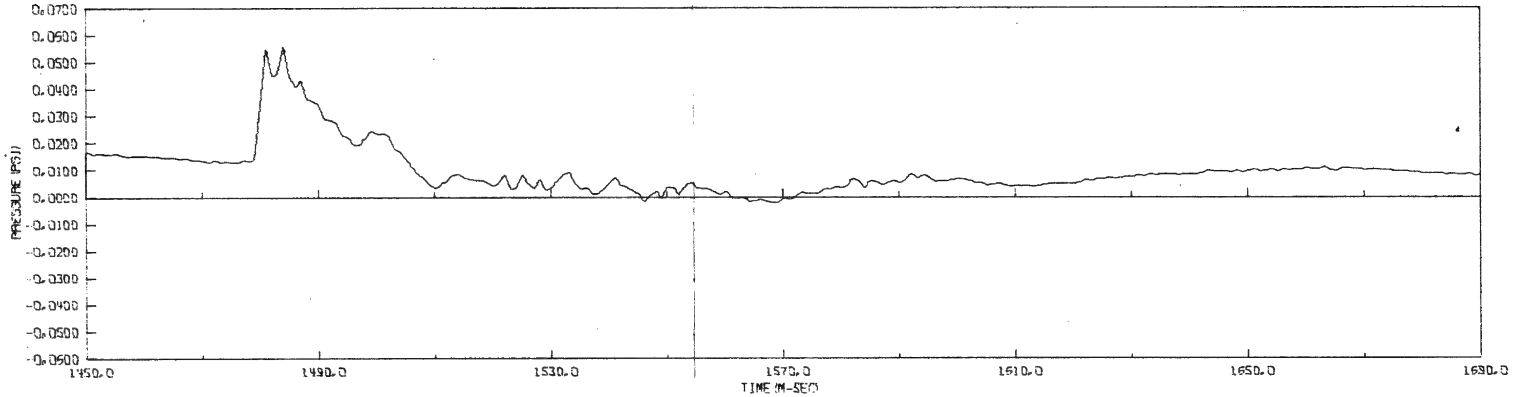

Figure A-13 Expanded pressure-time records of flare pulse from the station at 1575 feet (Gage 2)

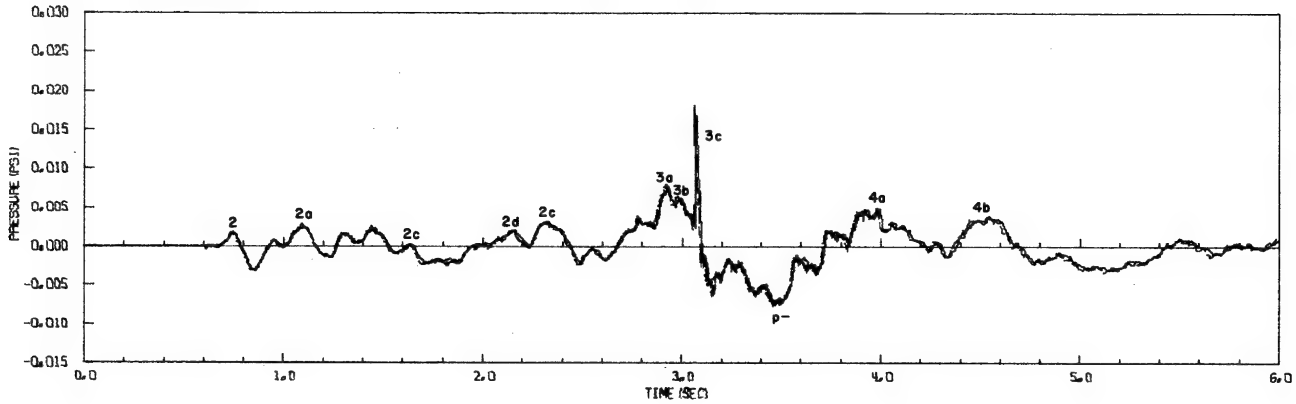

Figure A-14 Pressure-time records from the station at 3280 feet (2 gages)

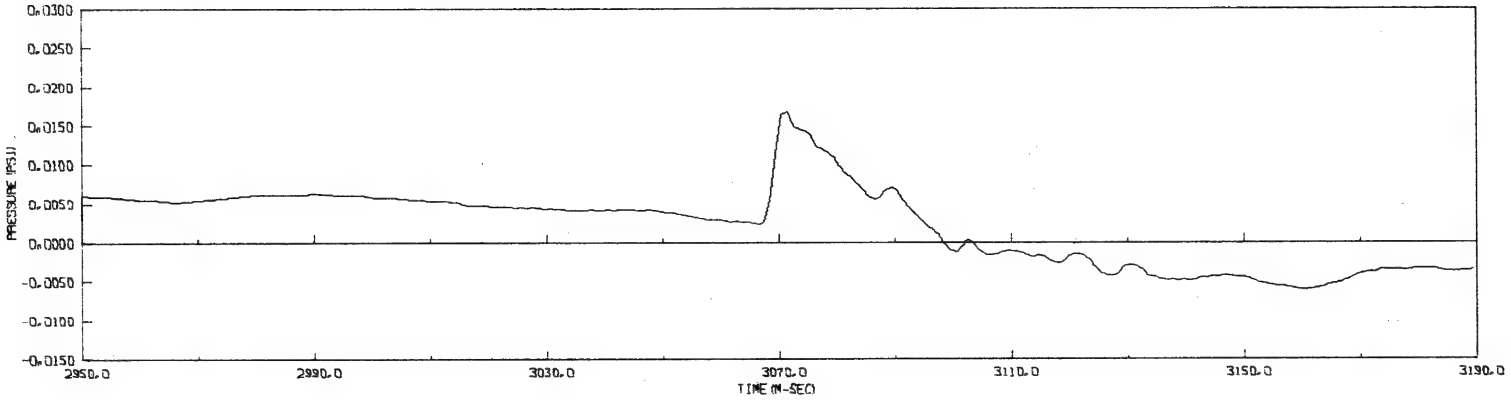

Figure A-15 Expanded pressure-time records of flare pulse from the station at 3280 feet (Gage 1)

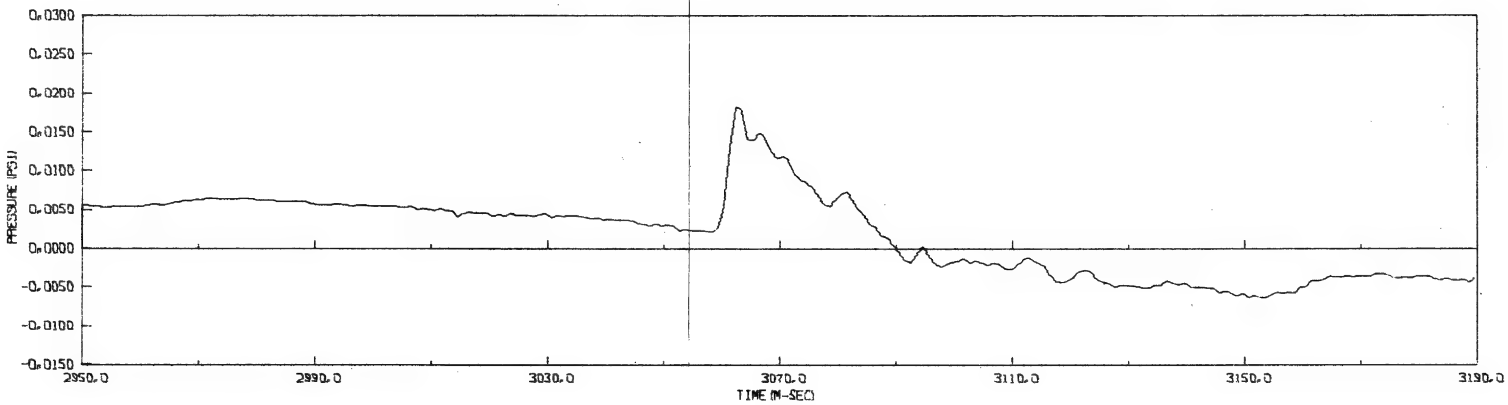

Figure A-16 Expanded pressure-time records of flare pulse from the station at 3280 feet (Gage 2)

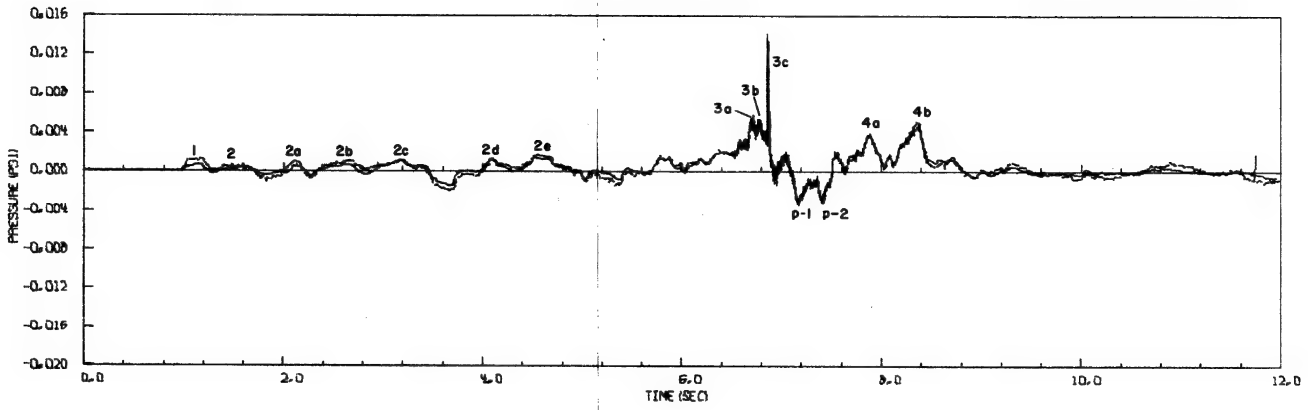

Figure A-17 Pressure-time records from the station at 7380 feet (2 gages)

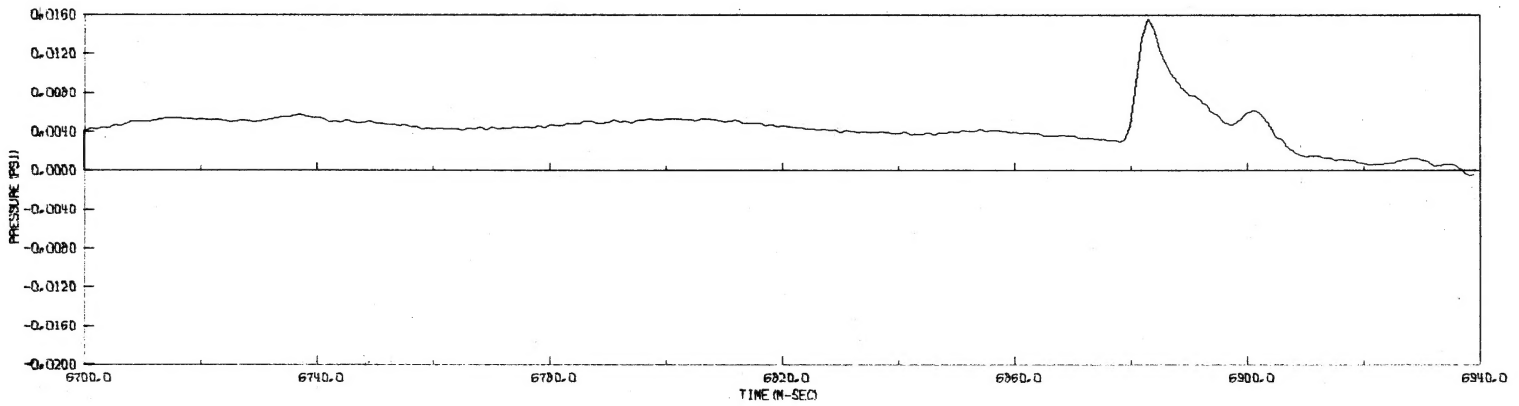

Figure A-18 Expanded pressure-time records of flare pulse from the station at 7380 feet (2 gages)

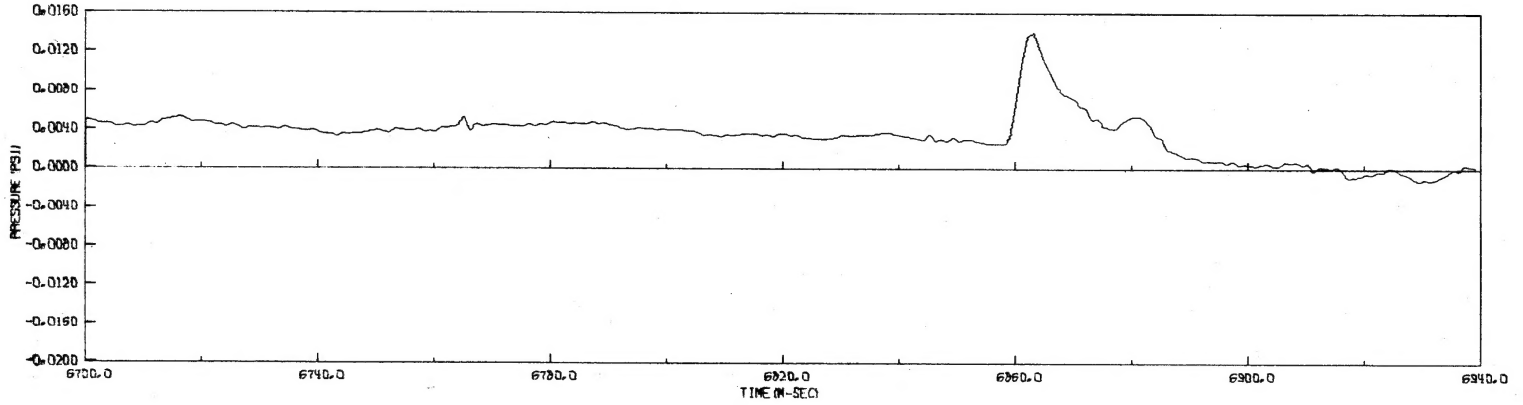

Figure A-19 Expanded pressure-time records of flare pulse from the station at 7380 feet (Gage 2)

PALANQUIN TECHNICAL REPORTS

Report No.	Agency	Author	Title
PNE-900F	LRL/EGG	R. Rohrer	Ground Motion and Cloud Photography
PNE-901F	LRL	C. Sisemore	Sub-Surface Effects
PNE-902F	SC	L. Vortman	Close-in Air Blast from a Cratering Nuclear Detonation in Rhyolite
PNE-903F	SC	J. Reed	Long-Range Air Blast
PNE-904F	NCG	F. Videon	Crater Topography
PNE-905F	NCG	P. Fisher	Pre-Shot Geological and Engineering Properties Investigations
PNE-906F	LRL/N	L. Meyer	Geophysical Studies
PNE-907F	LRL	T. Gibson et al	Hazards Evaluation Measurements
PNE-908F	EG&G, Inc.	R. Rohrer	Scientific Photography
PNE-909F	LRL	J. Miskel N. Bonner et al	Radiochemical Studies
PNE-910F	USPHS	J. Coogan	Off-Site Surveillance
PNE-911F	REECo	B. Ubanks	On-Site Radiological Safety
PNE-912F	USWB		Weather and Radiation Support Activities
PNE-913F	R. F. Beers Inc.	L. Davis	Analysis of Surface Seismic Data

DISTRIBUTION LIST
(TID-4500, Category UC-35)

No. Copies	
1	AEC ALBUQUERQUE OPERATIONS OFFICE
1	AEC BETHESDA TECHNICAL LIBRARY
25	AEC DIVISION OF PEACEFUL NUCLEAR EXPLOSIVES
1	AEC LIBRARY, WASHINGTON
1	AEC MISSION TO THE IAEA
5	AEC NEVADA OPERATIONS OFFICE
1	AEC NEW YORK OPERATIONS OFFICE
1	AEC PATENT OFFICE
5	AEC SAN FRANCISCO OPERATIONS OFFICE
1	AEC SAVANNAH RIVER OPERATIONS OFFICE
1	AEC SCIENTIFIC REPRESENTATIVE, BELGIUM
1	AEC SCIENTIFIC REPRESENTATIVE, ENGLAND
1	AEC SCIENTIFIC REPRESENTATIVE, JAPAN
1	AEROSPACE CORPORATION, SAN BERNARDINO (AF)
1	AIR FORCE AERO PROPULSION LABORATORY (APE)
1	AIR FORCE FOREIGN TECHNOLOGY DIVISION
1	AIR FORCE INSTITUTE OF TECHNOLOGY
1	AIR FORCE SCHOOL OF AEROSPACE MEDICINE
1	AIR FORCE WEAPONS LABORATORY
1	AMES LABORATORY (AEC)
1	ARGONNE NATIONAL LABORATORY (AEC)
8	ARMY ABERDEEN PROVING GROUND
1	ARMY CHIEF OF ENGINEERS
1	ARMY ELECTRONICS COMMAND
1	ARMY ENGINEER DIVISION
5	ARMY ENGINEER NUCLEAR CRATERING GROUP
6	ARMY ENGINEER WATERWAYS EXPERIMENT STATION
1	ARMY MATERIEL COMMAND
1	ARMY MEDICAL FIELD SERVICE SCHOOL
1	ARMY MEDICAL RESEARCH UNIT
1	ARMY MOBILITY EQUIPMENT RESEARCH AND DEVELOPMENT CENTER
1	ARMY NUCLEAR DEFENSE LABORATORY
1	ARMY PICATINNY ARSENAL
1	ARMY ROCKY MOUNTAIN ARSENAL
1	ARMY SURGEON GENERAL
1	ARMY WALTER REED MEDICAL CENTER
1	ATOMIC POWER DEVELOPMENT ASSOCIATES, INC. (AEC)
2	ATOMICS INTERNATIONAL (AEC)
1	BABCOCK AND WILCOX COMPANY, WASHINGTON (AEC)
2	BATTELLE MEMORIAL INSTITUTE (AEC)
1	BATTELLE-NORTHWEST (AEC)
1	BROOKHAVEN NATIONAL LABORATORY (AEC)
2	BUREAU OF MINES, BARTLESVILLE (INT)
1	BUREAU OF MINES, DENVER (INT)
1	BUREAU OF MINES, LARAMIE (INT)
6	BUREAU OF RECLAMATION (INT)
1	DEPARTMENT OF AGRICULTURE NATIONAL LIBRARY
1	DOD DASA LIVERMORE
1	DOD DASA RADIOBIOLOGY RESEARCH INSTITUTE
1	DOD DASA SANDIA
1	DOD DASA WASHINGTON
1	DU PONT COMPANY, AIKEN (AEC)
1	DU PONT COMPANY, WILMINGTON (AEC)
1	EG&G, INC., ALBUQUERQUE (AEC)
1	EG&G, INC., LAS VEGAS (AEC)
5	EL PASO NATURAL GAS COMPANY
8	ENVIRONMENTAL RESEARCH CORPORATION (AEC)
1	ENVIRONMENTAL RESEARCH CORPORATION, LAS VEGAS (AEC)
1	ENVIRONMENTAL SCIENCE SERVICES ADMINISTRATION, LAS VEGAS (COMM.)
1	ENVIRONMENTAL SCIENCE SERVICE ADMINISTRATION, MARYLAND (COMM.)
1	FRANKFORD ARSENAL (P-D LABS.)
1	GENERAL DYNAMICS/FORT WORTH (AF)
1	GENERAL ELECTRIC COMPANY, CINCINNATI (AEC)
1	GENERAL ELECTRIC COMPANY, SAN JOSE (AEC)
1	GEOLOGICAL SURVEY, DENVER
1	GEOLOGICAL SURVEY, FLAGSTAFF (INT)
1	GEOLOGICAL SURVEY, MENLO PARK (INT)
1	GEOLOGICAL SURVEY (PECORA) (INT)
1	GULF GENERAL ATOMIC INCORPORATED (AEC)
2	HOLMES AND NARVER, INC. (AEC)
1	HUGHES AIRCRAFT COMPANY, FULLERTON (ARMY)
1	INSTITUTE FOR DEFENSE ANALYSIS (ARMY)
1	ISOTOPES, INC. (AEC)
1	JET PROPULSION LABORATORY (NASA)
1	LAWRENCE RADIATION LABORATORY, BERKELEY (AEC)
4	LAWRENCE RADIATION LABORATORY, LIVERMORE (AEC)
2	LOS ALAMOS SCIENTIFIC LABORATORY (AEC)
5	LOVELACE FOUNDATION (AEC)
1	MATHEMATICA (AEC)
1	MUESER, RUTLEDGE, WENTWORTH AND JOHNSTON (AEC)
1	MUTUAL ATOMIC ENERGY LIABILITY UNDERWRITERS (AEC)
1	NASA JOHN F. KENNEDY SPACE CENTER
1	NATIONAL BUREAU OF STANDARDS (LIBRARY)
1	NATIONAL INSTITUTES OF HEALTH (HEW)
1	NATIONAL REACTOR TESTING STATION (INC) (AEC)
1	NAVY ATOMIC ENERGY DIVISION
1	NAVY OFFICE OF NAVAL RESEARCH (CODE 422)
2	NAVY ORDNANCE LABORATORY
1	NAVY ORDNANCE SYSTEMS COMMAND
1	NAVY POSTGRADUATE SCHOOL
1	NAVY RADIOLOGICAL DEFENSE LABORATORY
1	NAVY SHIP SYSTEMS COMMAND HEADQUARTERS
1	NRA, INC.
4	OAK RIDGE NATIONAL LABORATORY (AEC)
1	OCEANOGRAPHIC SERVICES, INC. (AEC)
1	OHIO STATE UNIVERSITY (OCD)
3	PUBLIC HEALTH SERVICE, LAS VEGAS (HEW)
1	PUBLIC HEALTH SERVICE, MONTGOMERY (HEW)
1	PUBLIC HEALTH SERVICE, ROCKVILLE (HEW)
1	PUBLIC HEALTH SERVICE, WINCHESTER (HEW)
1	PUERTO RICO NUCLEAR CENTER (AEC)
1	PURDUE UNIVERSITY (AEC)
1	RADIOPTICS, INC. (AEC)
2	REYNOLDS ELECTRICAL AND ENGINEERING COMPANY, INC. (AEC)
4	SANDIA CORPORATION, ALBUQUERQUE (AEC)
1	SANDIA CORPORATION, LIVERMORE (AEC)
1	SOUTHWEST RESEARCH INSTITUTE (AEC)
1	STANFORD UNIVERSITY (AEC)
1	TENNESSEE VALLEY AUTHORITY
1	UNION CARBIDE CORPORATION (ORGDP) (AEC)
1	UNIVERSITY OF CALIFORNIA, DAVIS, TALLEY (AEC)
1	UNIVERSITY OF MICHIGAN (VESIAC) (ARMY)
1	UNIVERSITY OF ROCHESTER (KAPLON) (AEC)
1	UNIVERSITY OF TENNESSEE (AEC)
1	UNIVERSITY OF WASHINGTON (AEC)
1	WASHINGTON STATE UNIVERSITY (AEC)
1	WESTINGHOUSE ELECTRIC CORPORATION, MC KENNA (AEC)
66	AEC DIVISION OF TECHNICAL INFORMATION EXTENSION
25	CLEARINGHOUSE FOR FEDERAL SCIENTIFIC AND TECHNICAL INFORMATION
296	

DISTRIBUTION LIST

1 D. J. Convey, Department of Mines and Technical Surveys, Ottawa, Ontario, Canada
1 Dr. G. W. Govier, Oil and Gas Conservation Board, Calgary, Alberta, Canada
1 U. S. Army Engineer Division, Lower Mississippi Valley, P. O. Box 80, Vicksburg, Mississippi 39181
1 U. S. Army Engineer District, 668 Federal Office Building, Memphis, Tennessee 38103
1 U. S. Army Engineer District, P. O. Box 60267, New Orleans, Louisiana 70160
1 U. S. Army Engineer District, 906 Olive Street, St. Louis, Missouri 63101
1 U. S. Army Engineer District, P. O. Box 60, Vicksburg, Mississippi 39181
1 U. S. Army Engineer Division, APO N. Y. 09019, Leghorn, Italy
1 U. S. Army Engineer District, GULF, APO N. Y. 09205, Teheran, Iran
1 U. S. Army Engineer Division, P. O. Box 103, Downtown Station, Omaha, Nebraska 68101
1 U. S. Army Engineer District, 1800 Federal Office Building, Kansas City, Missouri 64106
1 U. S. Army Engineer District, 6012 U. S. Post Office & Court House, 215 No. 17th Street, Omaha, Nebraska 68101
1 U. S. Army Engineer Division, 424 Trapelo Road, Waltham, Massachusetts 02154
1 U. S. Army Engineer Division, 90 Church Street, New York, New York 10007
1 U. S. Army Engineer District, P. O. Box 1715, Baltimore, Maryland 21203
1 U. S. Army Engineer District, 111 East 16th Street, New York, New York 10003
1 U. S. Army Engineer District, Ft. Norfolk, 803 Front Street, Norfolk, Virginia 23510
1 U. S. Army Engineer District, Custom House, 1nd & Chestnut Street, Philadelphia, Pennsylvania 19106
1 U. S. Army Engineer Division, 536 S. Clark Street, Chicago, Illinois 60605
1 U. S. Army Engineer District, Foot of Bridge Street, Buffalo, New York 14207
1 U. S. Army Engineer District, 219 S. Dearborn Street, Chicago, Illinois 60604
1 U. S. Army Engineer District, P. O. Box 1027, Detroit, Michigan 48231
1 U. S. Army Engineer District, Clock Tower Building, Rock Island, Illinois 61202
1 U. S. Army Engineer District, 1217 US PO & Customhouse, St. Paul, Minnesota 55101
1 U. S. Army Engineer District, Lake Survey, 630 Federal Building, Detroit, Michigan 48226
1 U. S. Army Engineer Division, 210 Custom House, Portland, Oregon 97209
1 U. S. Army Engineer District, 628 Pittock Block, Portland, Oregon 97205
1 U. S. Army Engineer District, P. O. Box 7002, Anchorage, Alaska 99051
1 U. S. Army Engineer District, 1519 Alaska Way, South, Seattle, Washington 98134
1 U. S. Army Engineer District, Building 602, City-County Airport, Walla Walla, Washington 99362
1 U. S. Army Engineer Division, P. O. Box 1159, Cincinnati, Ohio 45201
1 U. S. Army Engineer District, P. O. Box 2127, Huntington, West Virginia 25721
1 U. S. Army Engineer District, P. O. Box 59, Louisville, Kentucky 40201
1 U. S. Army Engineer District, P. O. Box 1070, Nashville, Tennessee 37202
1 U. S. Army Engineer District, 2032 Federal Building, 1000 Liberty Avenue, Pittsburg, Pennsylvania 15222
1 U. S. Army Engineer Division, Building 96, Fort Armstrong, Honolulu, Hawaii 96813
1 U. S. Army Engineer District, Far East, APO, San Francisco, California 96301
1 U. S. Army Engineer District, Building 96, Fort Armstrong, Honolulu, Hawaii 96813
1 U. S. Army Engineer District, Okinawa, APO, San Francisco, California 96331
1 U. S. Army Engineer Division, 510 Title Building, 30 Pryor Street SW., Atlanta, Georgia 30303
1 U. S. Army Engineer District, P. O. Box 1042, Merritt Island, Florida 32952
1 U. S. Army Engineer District, P. O. Box 905, Charleston, South Carolina 29402
1 U. S. Army Engineer District, P. O. Box 4970, Jacksonville, Florida 32201
1 U. S. Army Engineer District, P. O. Box 1169, Mobile, Alabama 36601
1 U. S. Army Engineer District, P. O. Box 889, Savannah, Georgia 31402
1 U. S. Army Engineer District, P. O. Box 1890, Wilmington, North Carolina 28402
1 U. S. Army Engineer Division, 630 Sansome Street, Room 1216, San Francisco, California 94111
1 U. S. Army Engineer District, P. O. Box 17277, Foy Station, Los Angeles, California 90017
1 U. S. Army Engineer District, 650 Capitol Mall, Sacramento, California 95814
1 U. S. Army Engineer District, 100 McAllister Street, San Francisco, California 94102
1 U. S. Army Engineer Division, 1114 Commerce Street, Dallas, Texas 75202
1 U. S. Army Engineer District, P. O. Box 1538, Albuquerque, New Mexico 87103
1 U. S. Army Engineer District, P. O. Box 1600, Fort Worth, Texas 76101
1 U. S. Army Engineer District, P. O. Box 1229, Galveston, Texas 77551
1 U. S. Army Engineer District, P. O. Box 867, Little Rock, Arkansas 72203
1 U. S. Army Engineer District, P. O. Box 61, Tulsa, Oklahoma 74102
1 U. S. Army Liaison Detachment, 111 E. 16th Street, New York, New York 10003
1 Mississippi River Commission, P. O. Box 80, Vicksburg, Mississippi 39181
1 Rivers and Harbors, Boards of Engineers, Temp C Building, 2nd & Q Streets SW., Washington, D. C. 20315
1 Corps of Engineer Ballistic Missile Construction Office, P. O. Box 4187, Norton Air Force Base, California 92409
1 U. S. Army Engineer Center, Ft. Belvoir, Virginia 22060
1 U. S. Army Engineer School, Ft. Belvoir, Virginia 22060
1 U. S. Army Engineering Reactors Group, Ft. Belvoir, Virginia 22060
1 U. S. Army Engineer Training Center, Ft. Leonard Wood, Missouri 65473
1 U. S. Coastal Engineering Research Board, 5201 Little Falls Road NW., Washington, D. C. 20016
75 U. S. Army Engineer Waterways Experiment Station, Vicksburg, Mississippi 39180
50 U. S. Army Engineer Nuclear Cratering Group, Livermore, California 94551